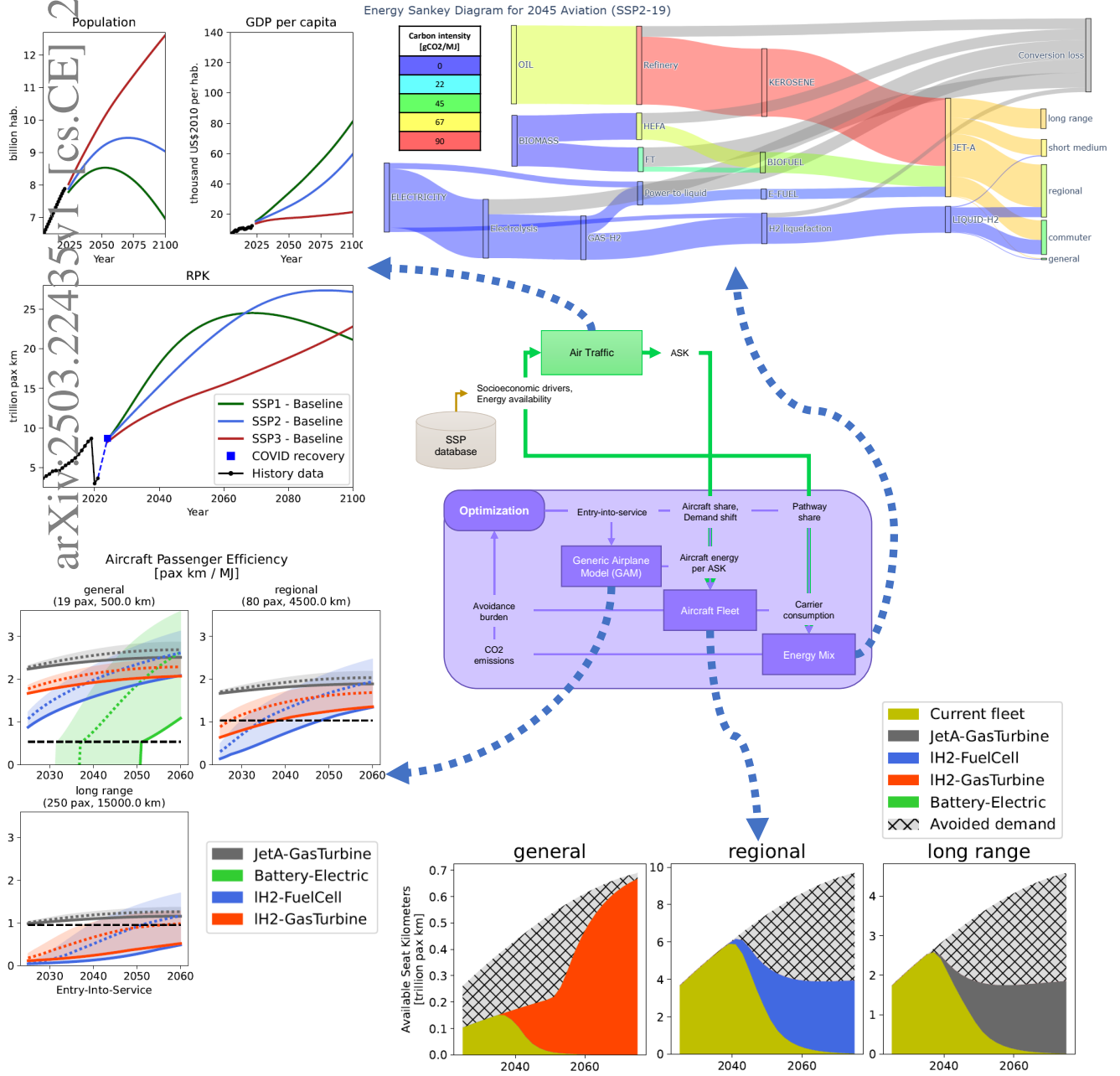


Graphical Abstract

Numerical optimization of aviation decarbonization scenarios: balancing traffic and emissions with maturing energy carriers and aircraft technology

Ian Costa-Alves, Nicolas Gourdain, François Gallard, Anne Gazaix, Yri Amandine Kambiri, Thierry Druot



Highlights

Numerical optimization of aviation decarbonization scenarios: balancing traffic and emissions with maturing energy carriers and aircraft technology

Ian Costa-Alves, Nicolas Gourdain, François Gallard, Anne Gazaix, Yri Amandine Kambiri, Thierry Druot

- Technology maturing greatly affects performance of alternative aircraft designs;
- Under trend demand, emissions peak by 2040, regardless of future fleet and energy availability;
- Paris Agreement targets will require demand management or extra energy availability;
- Aircraft with alternative energy carriers allows for better use of energy resources;
- Scientific computing libraries allowed for lighter implementation and faster execution.

Numerical optimization of aviation decarbonization scenarios: balancing traffic and emissions with maturing energy carriers and aircraft technology

Ian Costa-Alves^{a,b,*,1}, Nicolas Gourdain^a, François Gallard^b, Anne Gazaix^b, Yri Amandine Kambiri^{a,c} and Thierry Druot^c

^aAerodynamics, Energetics and Propulsion Department, ISAE-SUPAERO, 10 av. Marc Pégélin, Toulouse, 31055, France

^bMultidisciplinary Optimization Competence Center, IRT Saint Exupéry, 3 rue Tarfaya, 31400, Toulouse, France

^cConceptual Airplane Design and Operations, ENAC, 7 av. Marc Pégélin, Toulouse, 31400, France

ARTICLE INFO

Keywords:

Multidisciplinary Optimization
Low-carbon fuels
Aircraft design
Integrated Assessment Models
Shared Socioeconomic Pathways

ABSTRACT

Despite being considered a hard-to-abate sector, aviation's emissions will play an important role in long-term climate mitigation of transportation. The introduction of low-carbon energy carriers and the deployment of new aircraft in the current fleet are modeled as a technology-centered decarbonization policy, and supply constraints in targeted market segments are modeled as demand-side policy. Shared socioeconomic pathways (SSP) are used to estimate the trend traffic demand and limit the sectoral consumption of electricity and biomass. Mitigation scenarios are formulated as optimization problems and three applications are demonstrated: single-policy optimization, scenario-robust policy, and multi-objective policy trade-off. Overall, we find that the choice of energy carrier to embark is highly dependent on assumptions regarding aircraft technology and background energy system, and that aligning trend scenarios with the Paris Agreement market-targeted traffic constraints are required to align trend scenarios with the Paris Agreement. The usual burdens associated with nonlinear optimization with high-dimensional variables are dealt with by jointly using libraries for Multidisciplinary Optimization (GEMSEO) and Automatic Differentiation (JAX), which resulted in speedups of two orders of magnitude at the optimization level, while reducing associated implementation efforts.

1. Introduction

Air transportation is often considered a hard-to-abate sector, because carbon-free commercial aircraft are not readily available, and the production of alternative energy carriers on a global scale requires significant amounts of biomass and low-carbon electricity to meet the growing demand [1]. However, the sector will play a critical role in long-term climate mitigation of transportation [2].

Several key energy carriers have emerged as potential substitutes of conventional kerosene, such as synthetic kerosene (from biomass-to-liquid or power-to-liquid pathways), liquid hydrogen, ammonia, liquid natural gas, ethanol, methanol, and batteries [3]. Among these, only synthetic kerosene can be used in today's fleet without aircraft redesign. Current engines are limited by certification to a 50 % mixing ratio with conventional kerosene, but there is ongoing advances on the operation with 100 % Sustainable Aviation Fuels [4].

Compared to ground and marine transportation vehicles, aircraft are more weight sensitive because they must generate lift in order to remain airborne. Increasing mass leads to an increase in induced drag, which further increases the structural mass to support extra loads, leading to more drag, and so on. This snowball effect is a central phenomenon in

the conception of aircrafts [5], which means that estimating energy consumption is a fundamentally coupled problem. Alternative aircraft designs, flying with different energy carriers, may display higher energy consumption and/or limited payload and ranges compared to conventional jet-fueled planes, due to low specific energy (batteries) or due to the need for heavier cryogenic fuel tanks (liquid hydrogen).

"Since the IPCC's Fifth Assessment Report (AR5) there has been a growing awareness of the need for demand management solutions combined with new technologies, such as the rapidly growing use of electromobility for land transport and the emerging options in advanced biofuels and hydrogen-based fuels for shipping and aviation." [6, Executive Summary]

Integrated Assessment Models (IAM) are the tools used to simulate the evolution of the coupled climate-energy-land system from socioeconomic assumptions on climate mitigation and adaptation. Since the publication of the Shared Socioeconomic Pathways (SSP) [7], great improvements have been made in the detail given to transportation modes within global mitigation. The modeling of aviation within IAM's, has shown how demand-side measures may play an important role in keeping temperature increase between 1.5 and 2° C above preindustrial levels [8], but also how the incorporation of synthetic kerosene and the deployment of new aircraft with alternative energy carriers (such as hydrogen and biofuels) can also play a significant role in reaching stringent targets [9, 10].

 ian.costa-alves@isae-supaero.fr (I. Costa-Alves);
nicolas.gourdain@isae-supaero.fr (N. Gourdain);
francois.gallard@irt-saintexupery.com (F. Gallard);
anne.gazaix@irt-saintexupery.com (A. Gazaix)
ORCID(s): 0009-0009-4458-6641 (I. Costa-Alves)

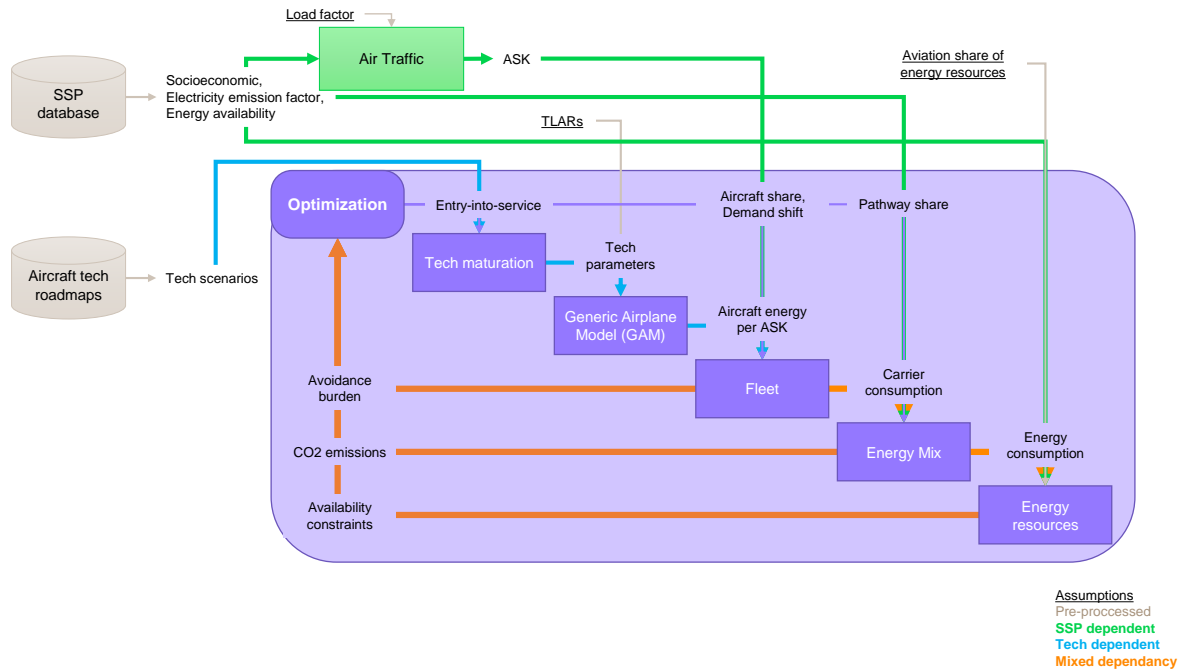


Figure 1: Conceptual view of the optimization process and data-flow between modeled disciplines.

However, the detail these studies have concerning the fleet composition and how they are arranged within market segments is limited, e.g., [10] considers kerosene, electric, and hydrogen aircraft to have similar energy consumption even for long-haul (where electric is unfeasible, and hydrogen is less efficient), while [9] accounts for lower efficiencies for hydrogen, it does so with a singular value applied for the entire fleet. The performance of hydrogen aircraft is highly dependent on their range and the cryogenic tank technology [11], which can lead to increased energy consumption [12] or limited operation in terms of payload and ranges [13]. For electric aircraft, this is even more pronounced as the battery weight significantly shortens the maximum achievable range and payload, making these aircraft only suited to regional flights [14].

Sectoral specific scenarios can account for this either with a detailed network of Origin-Destination pairs [15, 16, 17], or by separating the traffic into market segments according to flown distance. A review of sectoral aviation scenarios [18] shows that methodologies may differ regarding: traffic evolution, mitigation levers, inclusion of non-CO₂ effects, and resource consumption. Employing open-source tools [19] to simulate these types of scenarios can be greatly beneficial to explicit modeling assumptions and finding a common ground for high-level decision making.

This work builds on the literature of aviation climate mitigation scenarios by linking sectoral mitigation with a background system based on the Shared Socioeconomic

Pathways (SSP) using the AR6 scenario database [20]. Socioeconomic drivers are used to estimate future traffic volumes, based on the assumption that historical trends on traffic growth from personal income and population growth remain unchanged. Biomass and electricity consumed by scenarios are limited by using the concept of a fair share of global production that is allocated to the sector, which avoids over-consumption that can be detrimental to other economic sectors [1].

This methodology was introduced in [21], which addressed the exploration of technology-based decarbonization scenarios with optimization algorithms. Novel developments include the incorporation of demand avoidance strategies, the timing of introduction of new technologies, multi-objective optimization strategies, and multi-scenario simulations, which allowed to address Pareto-optimal trade-offs between demand-side and technology-centered measures, and also the robustness to a change in global scenario.

It is important to note that the generated scenarios are considered as decarbonization scenarios rather than climate mitigation scenarios, because non-CO₂ emissions are unaccounted for. While these effects can make up for more than half of aviation's contribution to global warming in the 2000-2018 period [22], there are still significant uncertainties concerning their estimation, especially when considering novel propulsion systems, for which little data is available. Furthermore, because of the short-lived nature of these warming effects, the debate on which metrics to use for comparing them to CO₂ is still ongoing [23]. However, some findings indicate that designing aircraft to fly lower

and slower is capable of significantly reducing non-CO₂ effects, with little extra fuel and cost penalties [24], these are incorporated in the aircraft design requirements (subsection 2.3).

While the usage of optimization within IAM's is not new [25, 26, 27, 28], there are several limitations with the tools used to solve them, which often imply a simplification of the problem: reducing time resolution, linearization of the problem [29], or even simplification of two-way couplings [30]. Multidisciplinary Optimization (MDO) frameworks can offer methods that allow for: formalizing the coupled problem within optimization routines, and using gradient-based algorithms, which allows nonlinear optimization to scale well despite increasing number of variables. On this methodological front, the present work also contributes to the formulation of optimal mitigation policies, and to alleviate the main drawback of using IAM's with MDO: the extra implementation burden, which is dealt with by using libraries with automatic differentiation capabilities.

The paper is organized as follows: first the quantitative models used are described and compared with the state-of-the-art, secondly the methodology behind optimal scenario formulation and implementation are discussed and initial computational gains are presented, then results of elementary models and optimal mitigation scenarios are presented and analyzed, the shortcomings of models are made explicit in the limitations section, and a critical view on the results and implications from the modeled future are addressed in the discussion, and finally the conclusion on the contributions this research brings are made.

2. Models

An overview of the data-flow between the model disciplines is presented in Figure 1. Before the optimization loop starts, the chosen global scenario determines the evolution of socioeconomic drivers (population and economy) and energy system (global production of biomass and electricity, and emission factor of grid electricity).

First, trend scenarios of air traffic demand and supply are generated from socioeconomic drivers, linked to a global scenario in the AR6 database [20].

Then, given the set of optimization variables, the time-dependent controls are solved, and the aircraft share, pathway share, and demand shift are obtained.

Aircraft energy consumption is estimated using an aircraft design model for a set of propulsion architectures and market segments, accounting for technology available by entry-into-service (EIS). Covered propulsion systems in this study are:

- Gas turbines powered by Jet-A
- Gas turbines powered by liquid hydrogen (LH₂)
- Electric propulsion powered by batteries
- Electric propulsion powered by liquid hydrogen and fuel cells

The final consumption of energy carriers are estimated per each market, accounting the operation of a bottom-up aircraft fleet, and a part of trend demand that is not met due to demand avoidance policy.

The primary energy consumed to meet the necessary carrier production and the emissions generated are estimated from process efficiencies, direct emissions from pathway production (used to simplify biofuels modeling) and grid electricity emission factor (used to model hydrogen production, liquefaction, and electrofuels) linked to a global scenario.

Finally, the primary energy consumption is constrained using the concept of an allocated share of global production of energy resources (biomass and electricity). As the choice of allocated resources dedicated to aviation is ultimately an outcome of political and market mechanisms, two different values are considered to explore the consequences of trend and extra energy availability.

The modeling of costs (energy, aircraft, operations) is outside the scope of this paper. Under the current production system, the price of alternative energy carriers is higher than that of fossil kerosene [31, 32], but this gap is expected to decrease in the near future due to scaling of production and due to carbon pricing [33], especially in scenarios with ambitious climate targets.

2.1. Time-dependent controls

First-order delays are commonly used to account for simplified inertia regarding: measuring and reporting information, receiving information and decisions being made, and even for decisions to have a visible effect on the state of a system [34, 35]. While the present work automates decision-making based on system outcomes, we still account for delays regarding the outcomes of time-dependent optimization variables (here called controls). Furthermore, this also allowed for numerical benefits, such as reduced dimensionality and improved the optimization stability.

Each output variable $o(t)$ is modeled as an Ordinary Differential Equation (Eq. 1), which is dependent on a given input variable $i(t)$ and a delay-time τ . Figure 2 shows the output response of the first-order delay system for a set of inputs. For the step and ramped step inputs (with ramp duration of 2τ), it takes 4τ and 5τ , respectively, for the output to reach 98 % of the step value. For the pulse, it takes 5τ to reach 2 % of the pulse value.

$$\frac{d}{dt}o(t) = \frac{i(t) - o(t)}{\tau} \quad (1)$$

The supply shift ratio (Eq. 8) and the shares of pathway production (Eqs. 12 and 14) are modeled with inputs that are coarsely discretized in time (5 years, while the simulation step is 2 years), here the input values at each time are optimization variables. The shares of aircraft market penetration are modeled with a ramp-up input, parameterized from 2 optimization variables (ramp start and max value) and a fixed parameter (ramp-up duration).

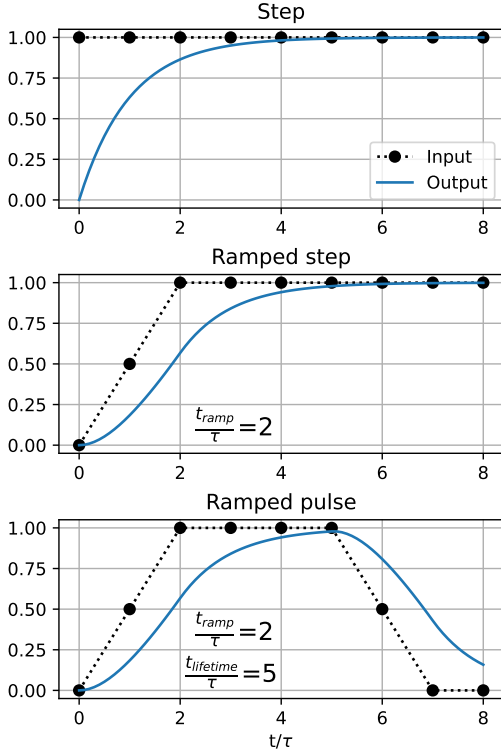


Figure 2: Output response of the first order delay to a set of inputs, subject to initial value of 0.

2.2. Air traffic demand

Many drivers can be linked to the growth in air traffic demand: population, disposable income, trade volumes, fuel prices, urbanization [37].

Equation 2 presents the model used in the Global Change Analysis Model (GCAM) [38, 27], where Pop is population, I is per-capita income, P is ticket price, ϵ_v is the elasticity of demand to variable v , and σ is a calibration constant.

$$D = \sigma Pop I^{\epsilon_I} P^{\epsilon_P} \quad (2)$$

Yet, there are several issues with using constant elasticities for forecasting aviation demand over long time-horizons. Meta-analyses categorize it as a luxury good and immature market [39], and post-COVID studies demonstrate how income elasticities may change rapidly depending on the state of the business cycle (normal, downturn, recovery) [40].

In the context of general transportation, these models are also limited to account for demand saturation as personal incomes rise, resulting in ever-growing demand volumes as the Gross Domestic Product (GDP) grows, and that by using S curves¹, to account for the income effect, can produce better estimates for both developed and developing countries [41]. This method was first applied for estimating personal vehicle stocks from personal income [42]. Results show that income elasticities can vary significantly as countries develop, but one shortcoming of the model is ignoring the effect of prices in modifying the demand.

¹Logistic, Gompertz, or Richards sigmoid functions.

In order to account for the phases of growth, maturation and saturation observed in aviation demand [43], a generalized logistic function is used to estimate trend per-capita demand from per-capita income. In Equation 3, L and R are the left and right asymptotes (personal propensity to travel at 0 and ∞ personal income), ι is the income per capita at the inflection point, B is the logistic growth rate, C controls the duration of the transition from L to R , and ν controls near which asymptote maximum growth occurs ($\nu = 1$ would yield an logistic equation and $\nu \rightarrow 0^+$ would tend to a Gompertz function).

$$RPK_{pc_{trend}}(t) = L + (R - L) \left(\frac{C}{C + e^{-B(I(t) - \iota)}} \right)^{1/\nu} \quad (3)$$

$$RPK_{trend}(t) = Pop(t) RPK_{pc_{trend}}(I(t)) \quad (4)$$

The parameter set $\theta = (L, R, \iota, B, C, \nu)$ must be calibrated with historical data. In Figure 3, World Bank data [36] provided for the demand (carrier departures), population, and income proxies on a regionalized level. But as the traveled distance is highly important in determining total emissions, in the present work, mitigation scenarios are driven by RPK demand, therefore ICAO data was used and calibrated on a global level over the 1980-2019 period. COVID years were excluded from the calibration data, and its after-effects were considered by assuming that by 2024 per capita traffic will reach 2019 levels, this is achieved shifting the parameter ι by the gap in income per capita between 2024 and 2019.

The supply, in terms of ASK, is then estimated using Load Factor (Eq. 5) that grows following a quadratic curve in time [44] from 82.4 % in 2019 to 92 % in 2075.

$$\text{Load Factor}(t) = RPK_{trend}(t) / ASK_{trend}(t) \quad (5)$$

2.3. Aircraft design

Modifying the energy carrier changes and the propulsion system architecture requires specific technology, e.g., cryogenic fuel tank, fuel cells, electric motors, all of which are expected to mature at different rates. To demonstrate this, several sources² are used to provide technology parameters and expected year of entry-into-service. Then, conservative-to-optimistic technology scenarios are made by interpolating the higher or lower bound of parameters in time.

Table 1 present the lower and upper values used for the technology parameters, according to entry-into-service (EIS) and Figure 4 displays how some key parameters are interpolated in time and how they compare with the sources used. The main goal of this is to be able to account for the trade-off regarding the timing of deployment of aircraft

²Sources include research papers on green hydrogen for transportation [45] technology roadmaps from IATA [46] and ATI [47, 48, 49, 50], ICCT aircraft design studies [12, 14, 13] NASA electric propulsion studies and technology aspiration [51, 52, 53, 54] and EASA type certificate data [55].

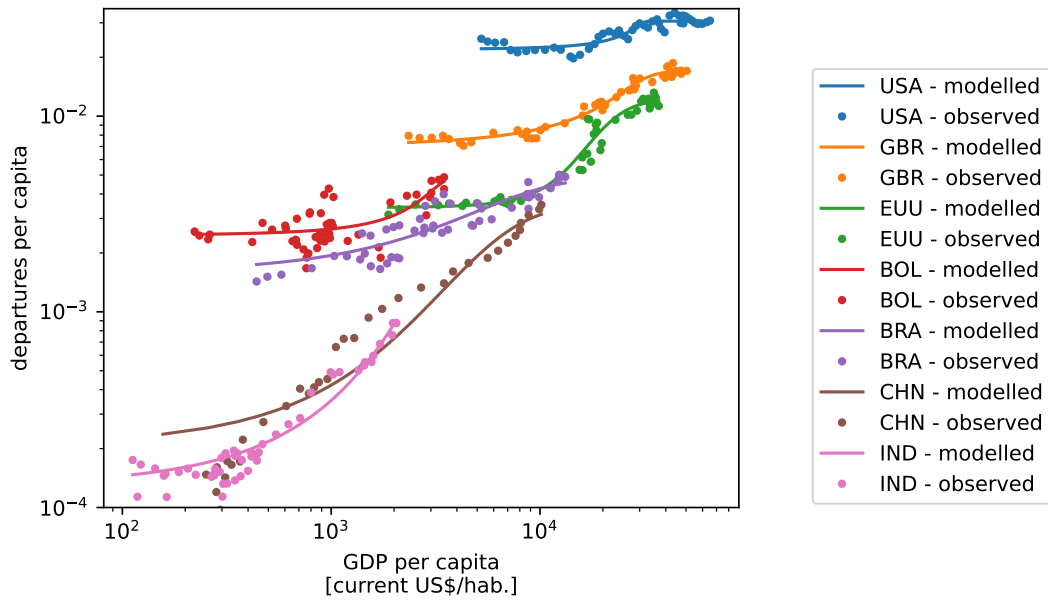


Figure 3: Regional calibration of registered carrier departures per capita as a generalized logistic function of income per capita. Region code: GBR - United Kingdom, USA - United States of America, EEU - European Union, BOL - Bolivia, BRA - Brazil, CHN - China, IND - India. Data from [36].

Table 1
Quantitative evolution of aircraft technology parameters.

Technology Parameter	Unit	2020	2040	2060	Sources
Battery Specific Energy	Wh/kg	200	350-700	600-1300	[46, 14, 51, 54, 53]
E-motor Specific Power	kW/kg	2	15-20	20-26	[49, 52]
Electronics Specific Power	kW/kg	2	15-22	20-30	[49, 53]
Fuel cell Specific Power	kW/kg	1	2-3	3-5	[46, 50, 52, 45]
Fuel cell Efficiency	%	40	45-50	50-60	[50, 45]
LH2 tank Gravimetric Index	%	20	30-60	40-75	[46, 48, 12, 13, 45]
Structural weight reduction	%	0	15-30	20-40	[46, 47]

Table 2
TLAR determined by market segment.

Category	Range (km)	Seats
General	500	19
Commuter	1500	50
Regional	4500	80
Short-medium	8000	120
Long range	15000	250

architectures: early deployment of maturing technology and lock-in with mediocre performance, or late deployment with mature and better performances.

In order to avoid technological optimism, especially in a sector that has historically missed most of its recent environmental targets [56], some sources that are systematically optimistic for the are purposefully left out of the technology scenario range.

The Top-Level Aircraft Requirements (TLAR) are split into two sets: the number of seats and range are determined solely by the market segment (Table 2), the cruise speed and

Table 3
TLAR determined by aircraft architecture.

Architecture	Speed (Mach)	Altitude (thousand ft)
Jet-A and Gas Turbine	0.75	27
LH2 and Gas Turbine	0.75	27
Battery and E-motor	0.5	20
LH2 fuel-cell and E-motor	0.5	20

altitude are determined by the propulsion architecture (Table 3). Overall, gas turbines can yield efficient operation at higher and faster flight conditions relative to propellers, but their cruise altitude and speed were purposefully limited in the present work, based on recent findings that re-designing aircraft to fly lower and slower can significantly reduce non-CO₂ impacts at less than 1 % extra operating cost [24, Figures 6.5, 6.8, 6.13, and Table E.4].

The Generic Airplane Model (GAM) [57], from ENAC, is then used as a preliminary airplane design tool. It uses regression of historical airplane data to estimate airframe

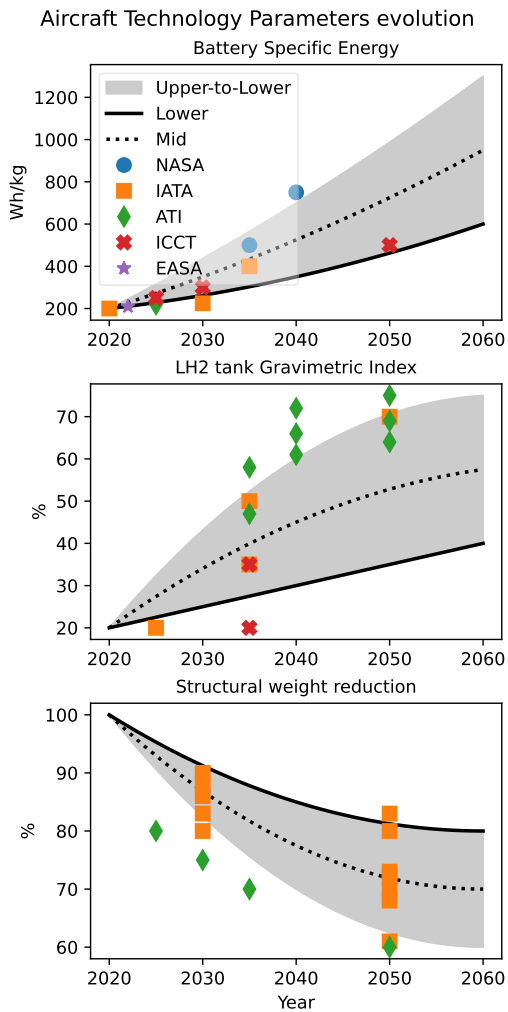


Figure 4: Improvement in selected aircraft parameters as a function of expected Entry-Into-Service. Filled between the upper and lower limit for the technology scenarios, solid line shows lower technology scenario, and dotted line shows mid technology scenario.

and structural weight and adds the propulsion system mass depending on the technology components that each architecture uses.

2.4. Fleet deployment

The global aircraft fleet is segmented into distance bands, rather than regionally or by routes. Figures 5 and 6 show, respectively, the 2019 repartition of ASK and emissions obtained from the AeroSCOPE database [58]. These are also used to compare the energy consumption of new aircraft designs.

Each market is assigned a constant share of trend supply, and subject to a demand-side policy that avoids part of the trend demand. The Supply-Shift Ratio SR is treated as a time-dependent control, whose input values are used as optimization variables in the low-demand formulation, and it represents the part of trend supply that is to be avoided (0: all trend supply is met, 1: all flights are banned).

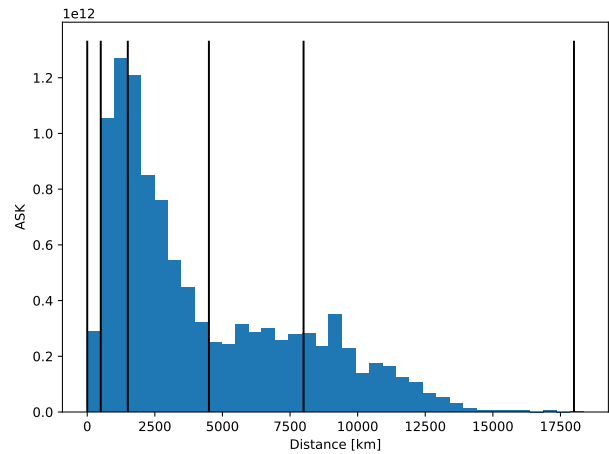


Figure 5: Histogram of the repartition of Available Seat-Kilometers according to flight distance of 2019 flights. Dark lines represent the repartition of distance among categories. Source: [58].

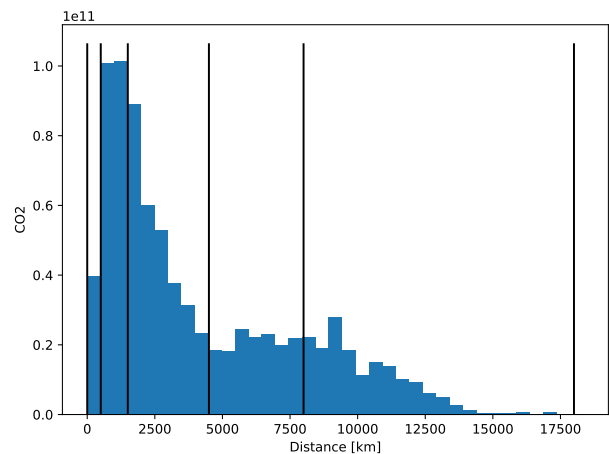


Figure 6: Histogram of the repartition of CO₂ emissions (kg) according to flight distance of 2019 flights. Dark lines represent the repartition of distance among categories. Source: [58].

In Equation 6, the annual burden associated to demand aversion is defined, formulated as the ratio between the volume of demand that is avoided and the volume of demand that is met. Under some strong simplifying hypothesis³, of constant price-elasticity and small price increase, it can be shown that this ratio is proportional to the relative ticket price increase felt by consumers. While the assumptions are not applicable to reality due to market-specific elasticities [59], they may still serve as simplified way to compare the suitability of scenarios with demand-aversion strategies without recurring to cost estimations.

³Under the assumptions that: demand reduction is achieved by pricing mechanisms, price elasticity is constant in time and among markets, and that price increases are sufficiently small. One can derive from the definition of price elasticity $\epsilon = \frac{dRPK/RPK}{dP/P}$ that the relative ticket price change is proportional to the relative demand change. By finding the mitigation scenario with minimal time-discounted relative demand reduction, the time-discounted relative ticket price increase is also minimized.

In Equation 7, the objective function of the low-demand formulation is defined as the present valuation of future policy burdens. It is a time-integration of the annual burden of demand avoidance, multiplied by a discount factor. The social discount rate d_f is the rate at which future burdens are undermined relative to present burdens, which was set at 4%. There is, however, a significant debate [60, 61] on whether this parameter should be defined by normative (how policies should be put in place) or positive (how policies likely will be put in place) approaches, the value chosen stands as a middle ground between the normative range 1.4-2.0% and the positive 5.0-6.6% range.

$$\theta_{avoidance}(t) = \left(\frac{\sum_{m \text{ in markets}} ASK_m(t) SR_m(t)}{ASK(t)} \right) \quad (6)$$

$$\Theta_{avoidance} = \int_{t_0}^{t_1} (1 + d_f)^{t_0-t} \theta_{avoidance}(t) dt \quad (7)$$

The market share of each aircraft type is also modeled using time-dependent controls (Eq. 1), but subject to a parameterized ramped pulse shape. The input signal is treated as zero before the year of Entry-Into-Service EIS, and then grows from 0 to a max share S_{max} linearly for a duration of t_{ramp} . EIS and S_{max} are tailored for each aircraft design and used as optimization variables. t_{ramp} is parameterized as $2\tau_{fleet}$ to maintain the ramped step shape (Fig. 2). and τ_{fleet} is kept as 4 years, meaning it takes 20 years from the introduction of a new aircraft to replace 98% of the fleet [62].

$$\begin{aligned} ASK(t) &= \sum_{m \text{ in markets}} ASK_m(t) \\ &= \sum_{m \text{ in markets}} S_m ASK_{trend}(t) (1 - SR_m(t)) \end{aligned} \quad (8)$$

The total energy carrier consumed by aircraft operations is estimated from covered supply and design energy consumption (sub-section 2.3) as shown in Equation 9. Then, the direct consumption of each energy carrier is aggregated as the sum among the carrier-consuming aircraft in Equation 10.

$$C_{aircraft_i}(t) = ASK_{aircraft_i}(t) EC_{aircraft_i} \quad (9)$$

$$C_{direct_energy} = \sum_{a \text{ in energy architectures}} C_a \quad (10)$$

2.5. Energy-Mix

This work considers different energy carriers, and for some of them several production pathways are available, such as synthetic fuels. Moreover, some energy carriers can be consumed in the production of other carriers and some of them can compete for the same primary energy sources

or materials. In that regards, it is necessary to consider a modular implementation to the energy production model.

Each energy conversion process is modeled in a modular manner as a production pathway. Pathways have a specific consumption of input flows per unitary production of output flows. The energy mix assembles all the production processes and the links them to calculate both intensive and extensive properties of the energy production system.

The computation of the impact generated (only CO2 emissions in this work, but any cumulative impact could be extended, such as land required, water consumption, ...) per unitary production, an intensive quantity, is made from primary-to-final⁴. This is mainly due to the fact that the impacts made in the production of inputs must be known beforehand in order to be accounted for in the indirect impacts of outputs.

On the other hand, the aggregated consumption and production of energies, an extensive quantity, is made from final-to-primary⁵, because total consumption of final energies determine the required consumption of inputs, which determines how much production of each energy-input is required.

In some implementations of modular energy system models, the estimation of properties is made altogether (intensive and extensive) per energy type and pathway [28]. This creates a coupled model (Figure 7): intensive quantities depend on the mix of the upstream system and extensive quantities depend on the aggregated consumption of the downstream system. This yields that an initial guess must be made up- and downstream, which is then iteratively solved until convergence. By separating modules responsible for estimating intensive and extensive quantities, if the system has no retroaction, the coupling disappears and direct computation can be achieved (Figure 8).

2.5.1. Intensive impacts

Impacts generated in the production of energy carriers are heavily dependent on the efficiency of processes and the impacts of consumed inputs, and these are mainly determined by the background energy system [67]. Recent works have highlighted the importance of linking global scenarios

⁴Consider the energy system required to produce two final energy carriers: Jet-A and liquid hydrogen. Jet-A is produced from a mix of fossil kerosene, and synthetic kerosene (electrofuel). Gaseous hydrogen is produced from electrolysis and is used to produce both liquid hydrogen, through liquefaction, and electrofuel, through power-to-liquid pathways. The emission factor (EF) of electrofuel and liquid hydrogen are both dependent on the EF of gaseous hydrogen, which depends on that of electricity. The computation of EF starts with electricity (primary), then gaseous hydrogen (secondary), then liquid hydrogen (final) and electrofuel (secondary), then Jet-A (final).

⁵The total production of each energy, however, must follow the inverse path: from final-to-primary. Taking the same example as footnote 4: Power-to-liquid production depends on Jet-A consumed, and liquefaction production depends on liquid hydrogen consumed. Electrolysis production depends on the gaseous hydrogen consumed in liquefaction and power-to-liquid production. Finally, electricity production required is estimated from consumption in the production of gaseous hydrogen. The computation of aggregated production and consumption starts with Jet-A (final) and liquid hydrogen (final), then electrofuel (secondary), then gaseous hydrogen (secondary), then electricity (primary).

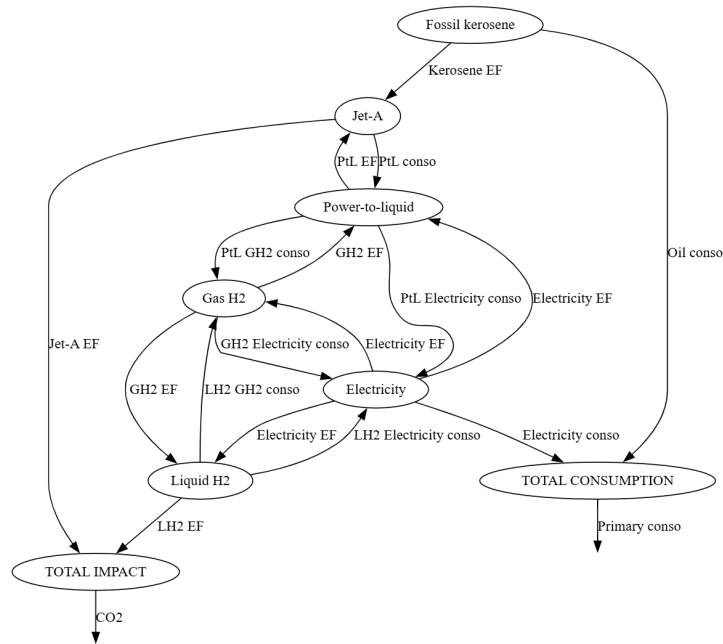


Figure 7: Coupling graph of the energy-mix models when using one module per energy type. This graph has two way couplings and require iterative processes to be solved.

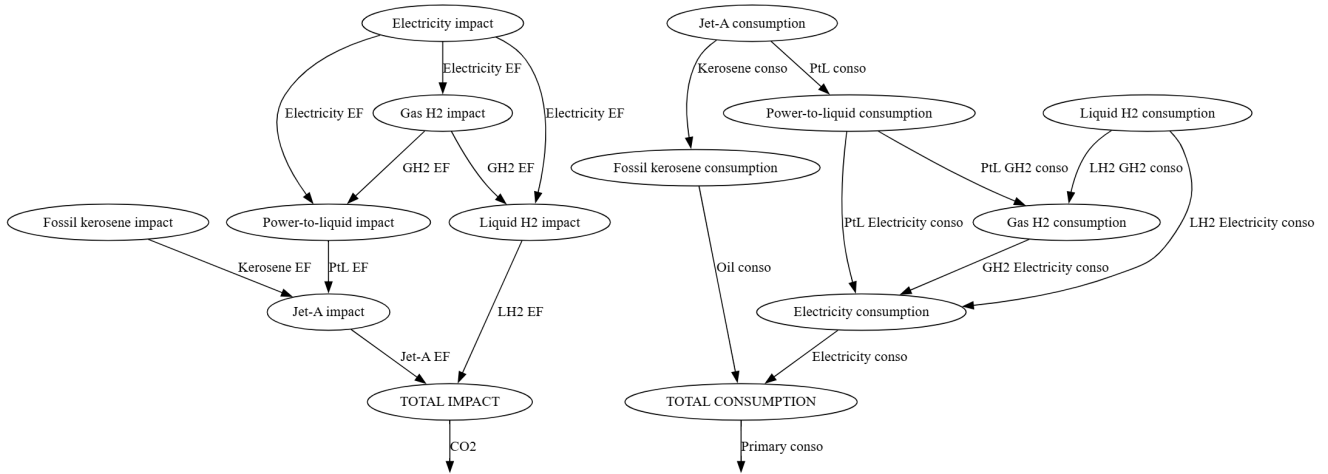


Figure 8: Coupling graph of the energy-mix models when using two modules (impact and consumption) per energy type. This graph has no two way couplings and can be solved sequentially.

to perform prospective life-cycle assessment of energy [68], and have also been applied for the prospective assessment of climate neutral aviation [69], showing a great increase in emissions associated with the production of synthetic jet fuel when a 3.5°C temperature increase scenario is chosen instead of a 2°C one.

The impact factor IF_{pathway} (Eq. 11), impact per unitary production, of each output flow associated to production pathways is modeled as the sum of direct impact generated at production plus the impacts associated to the input flows consumed in the process. $CF_{p,i}$ is the consumption of input i per unitary production of pathway p . This is made because

the inputs consumed in the process have impacts themselves, and by consuming them these indirect impacts must be accounted in the impacts of the output flow.

Table 4 summarizes the production pathways for each of the accounted energy carriers, their energy consumption and direct emissions per produced output. Technology maturing was accounted for some production pathways with an inverse consumption (analogous to process efficiency) that decreases linearly until stagnation in 2050. Table 5 summarizes the emission factor associated to the consumption of each energy input, such than total emissions are a sum of direct emissions and indirect emissions, and Figure 9 shows

Table 4

Energy consumption and direct emissions for each of the production pathways considered. For pathways under technology maturing, the two values represent the 2025 and 2050 values.

Energy Carrier	Production Pathway	Energy consumption (MJ/MJ)				Direct emissions (g CO ₂ / MJ)	Source
		Oil	Biomass	Electricity	Gas H ₂		
Fossil Jet-A	Refinery	1.16	-	-	-	15.5	[63, 64]
Biofuel	HEFA	-	1.95	-	-	62.73	[65]
	ATJ	-	3.33	-	-	51.55	
	FT	-	5.0	-	-	35.3	
Gas H ₂	Gas reforming	-	-	-	-	101.5	[66]
	Electrolysis	-	-	1.41-1.33	-	0	[45]
Electrofuel	Power-to-liquid	-	-	0.65-0.56	1.89-1.68;	0	
Liquid H ₂	Liquefaction	-	-	0.22-0.16	1.0	0	

Table 5

Emission factor associated to energy inputs and brief description of the method to estimate them. For pathways under technology maturing, the two values represent the 2025 and 2050 values.

Energy input	Emission factor (g CO ₂ / MJ)	Method	Source
Oil	63.32	Kerosene combustion divided by oil consumption	[64]
Biomass	0	Accounted only as biofuel direct emissions	[65]
Electricity	Scenario-dependent	Final consumption divided by electricity emissions	[20]

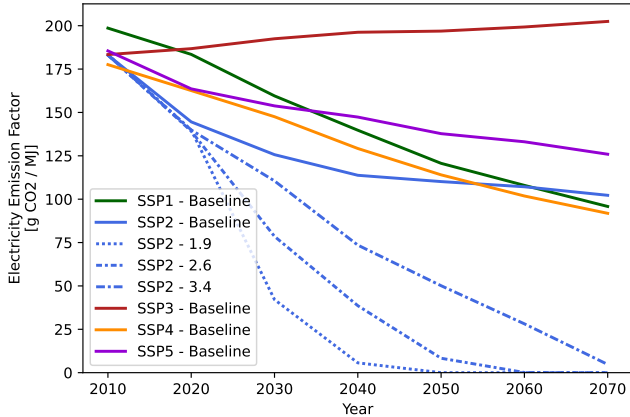


Figure 9: Emission factor associated to electricity consumption depending on the chosen background scenario. Source [20].

the electricity emission factor for electricity for a set of SSP background scenarios.

$$IF_{\text{pathway}} = IF_{\text{direct, pathway}} + \sum_{i \text{ in pathway inputs}} CF_{\text{pathway, } i} IF_i \quad (11)$$

Because each energy type can be produced by several pathways, a mixing process is applied where the energy mean impacts IF_{energy} (Eq. 12) is weighted by the share of pathway production, which are treated as a time-dependent control, used as optimization variables.

$$IF_{\text{energy}} = \sum_{p \text{ in energy pathways}} S_p IF_p \quad (12)$$

2.5.2. Extensive production and consumption

The production of each energy type (Eq. 13) is the direct energy consumption (directly embarked in aircraft) plus what was consumed to make other energy types. If e_0 is an energy input to e_1 , e_1 is an energy output to e_0 . The computation is initialized with final energies because the term $\sum_o (CF_{o,e} P_o)$ is zero, as no intermediate processes consume them.

$$P_{\text{energy}} = C_{\text{direct, energy}} + \sum_{o \text{ in energy outputs}} CF_{o, \text{energy}} P_o \quad (13)$$

$$P_{\text{pathway}} = S_{\text{pathway}} P_{\text{energy}} \quad (14)$$

$$C_{\text{pathway, input}} = CF_{\text{pathway, input}} P_{\text{pathway}} \quad (15)$$

$$C_{\text{energy, input}} = \sum_{p \text{ in pathways}} C_{p, \text{input}} \quad (16)$$

The production of each pathway (Eq. 14) is then estimated from pathway share. Input consumption of pathways are estimated (Eq. 15) and then are aggregated by energy type (Eq. 16). The process is then repeated for each energy type until primary energies.

2.5.3. Consumption and impacts constraints

For biomass and electricity, the total consumption is constrained applying the concept of an allocation principle, initially developed for Absolute Environmental Sustainability Assessments [70, 71], but applied for energy production (Equation 17). Because there is little consensus on how to find such fair shares [72], two different values were explored: one reflecting a conservative energy availability (5.0 %), and another reflecting a preferential availability to the aviation sector (8.6 %). Both values use some sort of grandfathering, which tend to lock the economic system into its present state. Yet, values are still conservative when compared to other institutional roadmaps, which can consume up to 9 % of available renewable electricity and 30 % of biomass [1].

The conservative value was obtained based on a reference mitigation scenario, the IMP-REN-2.0, in which 38.6 % of the biomass production is allocated to the transport sector [73, Figure 6.1], the fair share allocated to aviation is considered to be 13 % of that, which is the 2019 sector's share of oil consumption relative to the entire transportation consumption [74]. The preferential access value was obtained based on the sector's 2019 share of global oil consumption [74].

$$C_{\text{resource}} \leq s_{\text{resource}} P_{\text{resource}} \quad (17)$$

In the low demand formulation, the cumulative emissions of the sector is a constraint rather than the objective to minimize (Eq. 18). In these cases, we assumed the target carbon budget B_{carbon} to be the remaining 2°C carbon budget with 66 % confidence [75], and the fair share to be 3.0 %, which is the sector's share of direct, indirect and induced GDP [76].

$$\int_{t_0}^{t_1} CO_2(t) dt \leq s_{CO_2} B_{CO_2} \quad (18)$$

3. Numerical methods

3.1. Differential Programming for Multidisciplinary Optimization

Knowledge of new mitigation technology and climate sciences evolves constantly, therefore models also need to be continuously improved to account for new findings. As a consequence, the implementation burden associated to adding, modifying and extending models should be kept low.

The optimization of mitigation scenarios requires libraries that feature:

- Assembly and integration of numerous heterogeneous models;
- Scaling with high-dimensional variables, due primarily to the time-dependency, but also for uncertainty quantification and regionalization;
- Minimal extra implementation when incorporating or modifying models.

Multidisciplinary Optimization (MDO) frameworks are classically used to optimize or improve a given design under various constraints [77], it offers practical methods to handle model integration and coupling. Efficient optimization under high-dimension can also be achieved by using gradient-based algorithms, but their use often implies an extra burden due to the manual implementation of the derivatives of objective and constraints with regards to optimization variables. GEMSEO is an open-source Python software to automate multidisciplinary processes [78], which provided the following features that were used in the present study: automatic handling of coupled derivatives, automatic assembly of complex MDO processes based on dependency graphs, interfaces to optimization algorithms, results visualization, data storage.

Differential Programming, on the other hand, is commonly used for machine learning and scientific computing research. This programming paradigm allows for the Automatic Differentiation (AD) of lines of code. The use of AD for MDO can significantly reduce implementation burden associated to efficient high-dimension optimization. JAX is a library for array-oriented numerical computation, with capabilities for AD and just-in-time (JIT) compilation [79], enabling high-performance scientific computing in multiple hardware configurations (CPU, GPU, and TPU).

GEMSEO-JAX [80] is an open-source plug-in that was developed by the authors to bridge JAX programs into a GEMSEO process.

3.2. Single-objective optimization

Optimal mitigation policies are formulated as the general nonlinear programming problem, shown in Equation 19. Where the objective $f : \mathbb{R}^n \rightarrow \mathbb{R}$ and the constraint $\mathbf{g} : \mathbb{R}^n \rightarrow \mathbb{R}^m$ functions are assumed to be continuously differentiable, and the optimization variable \mathbf{x} is bound to lower (\mathbf{x}_{low}) and upper (\mathbf{x}_{up}) values.

$$\begin{aligned} & \min_{\mathbf{x} \in \mathbb{R}^n} f(\mathbf{x}) \\ & \text{subject to:} \\ & g_j(\mathbf{x}) = 0, \quad j = 1 \dots m_{\text{equality}} \\ & g_j(\mathbf{x}) \geq 0, \quad j = m_{\text{equality}} \dots m \\ & \mathbf{x}_{\text{low}} \leq \mathbf{x} \leq \mathbf{x}_{\text{up}} \end{aligned} \quad (19)$$

Two formulations of optimal mitigation scenarios are proposed: one relying on minimizing cumulative emissions by supplying for trend demand, while changing energy carriers and aircraft within the global fleet, here called trend formulation; and other that rather minimizes the supply aversion in order to align to a target cumulative emissions, here called low-demand formulation.

The optimization variables consist of aircraft mix parameters (EIS and S_{max} for each market and architecture type), energy mix parameters (control input values for the share of pathway production within each produced energy type), and, for the low-demand formulation, the supply cap parameters (control input values for the SR for each market). EIS is

bounded between 2035 and 2060, S_{\max} and the energy mix variables between 0 and 1, and SR between 0 and 0.6⁶ (at least 40 % of the trend demand is satisfied at each market).

The optimization constraints applied to all scenarios consist in limiting the sum of S_{\max} among aircraft types for each market to 1, limiting the share of pathway production to positive values among each produced energy, and limiting the consumption of biomass and electricity to a fixed fair share of the global production. Also, in the case where scenarios add electric aircraft to the fleet, an extra constraint on aircraft energy consumption is added to ensure designs are feasible by EIS.

In the trend formulation the objective function is the cumulative CO₂ emissions. In the low-demand formulation, cumulative emissions are constrained (Eq. 18), and the objective is the time-discounted burden of demand aversion (Eq. 7).

Numerical optimization is performed with the SLSQP Algorithm [81], using forward-mode AD to obtain the gradient of f and \mathbf{g} with respect to \mathbf{x} .

Forward-mode is chosen over reverse-mode, or back-propagation, due to the time-dependent nature of some constraints (share of pathway production and consumption of energy resources). In reverse-mode, a tape strategy has to be used, where intermediate values are stored in the memory and AD will trace the computation graph from them, this however yields a larger memory footprint [82]. One way to overcome this, is to perform time integration of constraint violation, reducing the dimension of outputs to differentiate, therefore lowering memory and computational footprint associated with backpropagation. When compared to forward-mode, this approach can lead to faster differentiation, but at the expense of the optimization convergence⁷ when multiple constraints are involved (which is the case here).

Robustness to background scenario

The robustness to the background scenario was also performed as a single-objective optimization problem. First a formulation must be chosen (results demonstrate the case for the trend formulation) and is performed in a multi-scenario simulation. The objective of the optimization problem is then considered as the mean of policy objectives under the scenario ensemble.

The optimization variables are then divided into two sets: one that is kept fixed among all scenarios (the aircraft mix variables), and one that may be specific to each scenario (the energy mix variables). This allows to ensure the robustness of the choice of aircraft mix while allowing for each scenario

⁶Considering a price elasticity of -0.6 [59], yields that a 1 % increase in ticket price yields 0.6 % reduction of demand. The 60 % threshold for supply aversion was chosen arbitrarily, corresponding to the hypothetical situation of doubling ticket prices.

⁷Time-integration of constraint violation is essentially viewed as a sum over a vectorized `if(g ≤ value)` statement, which is non-differentiable. When AD is applied over this operation it will compute a gradient that only accounts for the instants where the condition is true. This wrong approximation of the gradient of \mathbf{g} leads to an optimization that takes more iterations to reach the same level of convergence, or even fails to converge in some cases.

to individually optimize the energy production system in order to respect their respective availability constraints.

3.3. Traffic and emissions trade-off

The trade-off between mitigation policies with different objectives is formulated as a multi-objective problem. Differently to the single-objective formulation (Eq. 19), the scalar objective f is replaced by $\mathbf{f} : \mathbb{R}^n \rightarrow \mathbb{R}^k$, which is composed of k objectives. Instead of a single optimal solution, the goal of the optimization is to find a set of Pareto-optimal solutions, i.e., the set of compromises between the optima of each of the objectives.

Numerical optimization is performed with the ϵ -constraint method [83, 77], which converts the multi-objective problem into several single-objective sub-optimizations. The main idea is to keep only one of the objectives for the sub-problem and the others are converted into constraints, which are sampled into different values for each sub-problem.

3.4. Computational gains

In order to estimate the performance gains obtained by using a Differential Programming paradigm, we first compare execution time over an entire scenario optimization, then the comparison is made over a single computation and linearization.

In Table 6, an entire scenario optimization is performed with varying strategies with regards to the optimization algorithm, differentiation strategy, and compilation. First, by using gradient-based algorithms, not only the number of iterations required for convergence is significantly lowered, but also the precision of the objective value found is higher (lower objective value). This emphasizes the benefits of using such algorithms for problems with a high-dimensional optimization variables, which is already well known [84]. Secondly, using the un-compiled model with a Finite Differences (FD) differentiation method (standard) was prohibitive due to its memory and processing requirements, with JIT compilation and FD these become feasible, but still not as efficient (both in terms of number of iterations as in execution time) as using forward-mode AD. Overall, speedups of two order of magnitudes are achieved by using JAX for both algorithms tested.

In Table 7 the computation compares how long one single optimization loop (one scenario computation) takes to complete, with (JAX version) and without (standard) JIT compilation. The linearization compares how long it takes to differentiate objective and constraints with respect to the optimization variables, using JIT compiled forward-mode AD (JAX version) and without compilation (standard). JAX requires an extra overhead time of around 38 seconds at the first time a code is called, because compilation is just-in-time (JIT). This is excluded for the comparison of scenario computation and linearization, but are included in the comparison of scenario optimization. Overall, speedups of three order of magnitudes are achieved by using JAX, once the model is compiled.

Table 6

Benchmark over a single-objective scenario optimization with trend formulation. Performed using a single Intel(R) Core(TM) i7-10850H CPU core with 2.70 GHz, as the mean of 3 repetitions, varying technology assumptions. The objective (cumulative CO₂ emissions) is normalized by the 3% of the 2°C carbon budget.

Method	Algorithm	Gradient-based	Iterations	Total time (s)	Speedup	Objective value
Standard (FD)			X	X	X	X
FD + JIT	SLSQP	Yes	91	69.3	87	1.72
JAX version			86	53.2	114	1.72
Standard	COBYLA	No	1852	6052	-	1.75
JAX version			1898	51	119	1.75

Table 7

Benchmark over a single scenario computation and linearization. Performed using a mean of 50 repetitions in a single Intel(R) Core(TM) i7-10850H CPU core with 2.70 GHz.

Method	Computation (s)	Linearization (s)
Standard (FD)	372.7	362.6
JAX version	0.45	0.48
Speedup	830	749

For comparison, one scenario simulation using a restricted set of AeroMAPS [19] models (the default bottom-up simulation, excluding models for offsetting, non-CO₂, and cost estimation) takes 1.29 seconds to complete, around 3 times longer than using the present approach. This comparison must be taken with certain caution, due to the diverging scopes of each of them, for example the models in the present work account for: 5 market segments instead of 3, aircraft design routines, linkages between traffic growth and socioeconomic drivers, and a generic formulation of the energy production system.

4. Model and scenario results

4.1. Air Traffic Demand

Figure 10 shows the recent history and SSP scenario future evolution of Population and GDP per capita, and also the recent history and modeled future global RPK demand.

The high per capita GDP in SSP1 and 5 yield that personal propensity to travel stagnates, these scenarios also feature declining populations after 2050, which results in a global RPK demand that saturates around 2060.

Because the model is calibrated from historical trends, its suitability for forecasting disruptive scenarios is limited [41]. This is the case for SSP1, which diverts demand from energy-intense activities, and SSP3, with a resurgent nationalism and diverted focus from global to national issues [7]. Both scenarios are expected to display lower traffic volumes than the estimation provided by this model.

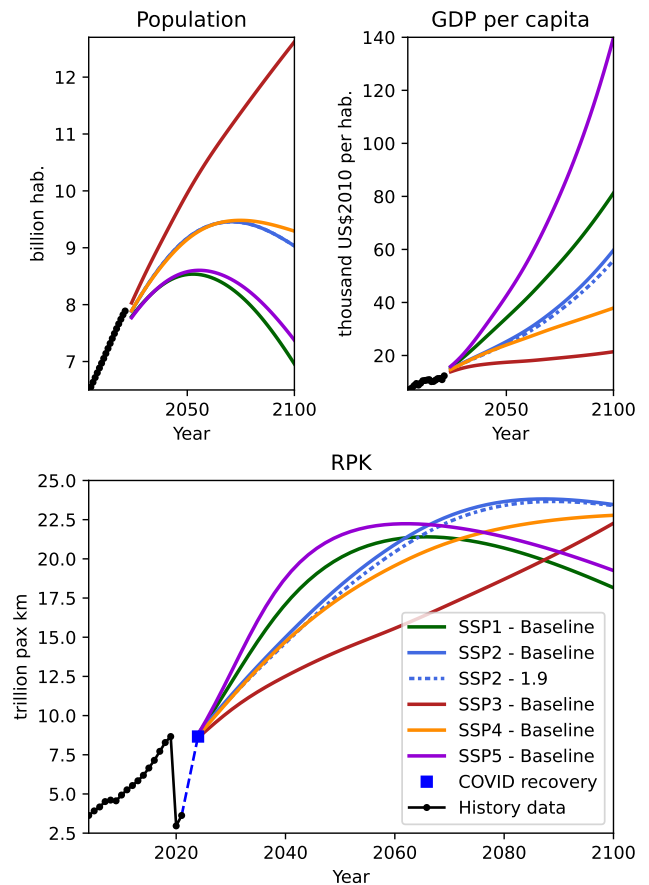


Figure 10: Historical evolution and modeled future global RPK demand from socioeconomic drivers linked to SSP scenarios.

4.2. Aircraft Design

Figure 11 shows the expected design performance of aircraft design architectures depending on prospective technology scenario. Energy consumption of new designs are compared with the 2019 mean consumption from commercial flight operated within the category distance bands, obtained from the AeroSCOPE dataset [58].

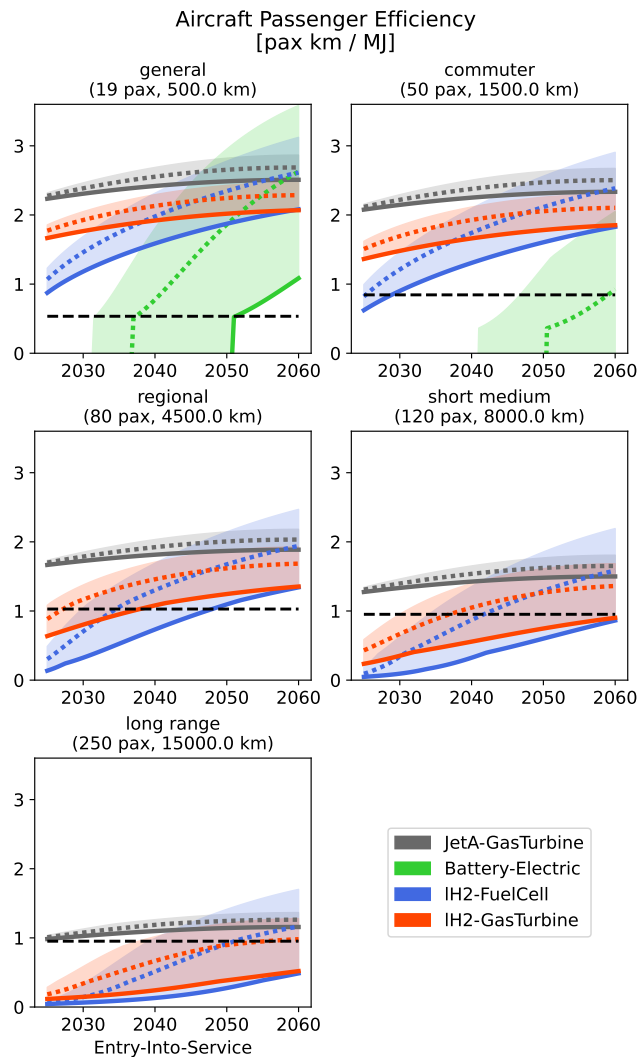


Figure 11: Expected passenger efficiency (inverse energy consumption) of prospective aircraft with technology available by Entry-Into-Service. Color-code is used to differentiate among aircraft architectures, filled between the upper and lower limit for the technology scenarios, solid line shows lower technology scenario, dotted line shows mid technology scenario. The black dashed line shows the performance of the 2019 mean fleet within the considered distance-bands [58].

Conventional aircraft

In general, new conventional gas turbine designs, powered by Jet-A perform better than the mean 2019 fleet, and this gap is wider over smaller distances. The diverging expectations in weight reduction expectations, yield a variation in the energy consumption of these designs depending on the chosen technology scenario, but this variation is relatively small compared to that of alternative designs.

Electric aircraft

Due to the low specific energy of batteries compared to other energy carriers, electric aircraft are still limited in range. Performance varies greatly with technology scenario,

due to variation of batteries, electric motors, and power electronics.

Low technology yields that feasible designs in the general market are only possible around 2050. With mid and upper technology, respectively, feasibility can be achieved by 2037 and 2032 in the general market, and by 2046 and 2038 in the commuter. By 2060, with upper technology, electric aircraft is the most efficient for the general market.

Hydrogen aircraft

Hydrogen aircraft are feasible across all markets regardless of EIS, both for architectures that burn hydrogen in gas turbines as for using them with fuel-cells and electric motors. Technology scenario affects them more than conventional aircraft, but less than electric. The sensibility regarding technology scenario is due to the gravimetric efficiency of liquid fuel tanks, but the fuel cell architecture displays higher sensitivity, also due to electric motors and fuel cells (both in terms of efficiency and specific power).

With lower technology, burning hydrogen in gas turbines is more efficient than using fuel cell for all markets, regardless of EIS. In the general and commuter market, as early as 2030 both are already more efficient than the reference 2019 aircraft. In the regional market, this shift happens by early 2034 and 2042, respectively. In the short-medium, by 2044 and 2050. But neither of them are able to reach 2019 efficiencies in the long-range even by 2050.

With mid technology, fuel cells surpass combustion around 2040, a bit earlier for shorter distances and a bit later for longer distances. Within the time-frame, both are able to surpass 2019 efficiencies, but neither are able to surpass the efficiency of turbofan architectures.

Finally, with upper technology hydrogen combustion is able to reach the lower-end of efficiency of conventional designs, but not the upper. Also with upper technology scenario, fuel cells are the most efficient option among architectures, except for the general market, but this supposes switching membranes with low temperature operation to high temperature [50].

4.3. Single policy optimization

The results of single-objective mitigation scenarios are presented. To showcase the impacts of aircraft with alternative energy carriers, two case-studies are presented and explored with varying technology scenarios: one with conventional aircraft, here called drop-in mitigation; and another with a mix of conventional and alternative aircraft, called breakthrough mitigation.

Each of them is further analyzed in 3 cases:

- Trend formulation (min CO₂), conservative energy allocation (5 % of global production);
- Trend formulation (min CO₂), preferential energy allocation (8.6 % of global production);
- Low demand formulation (min avoidance burden, constrained CO₂), conservative energy allocation.

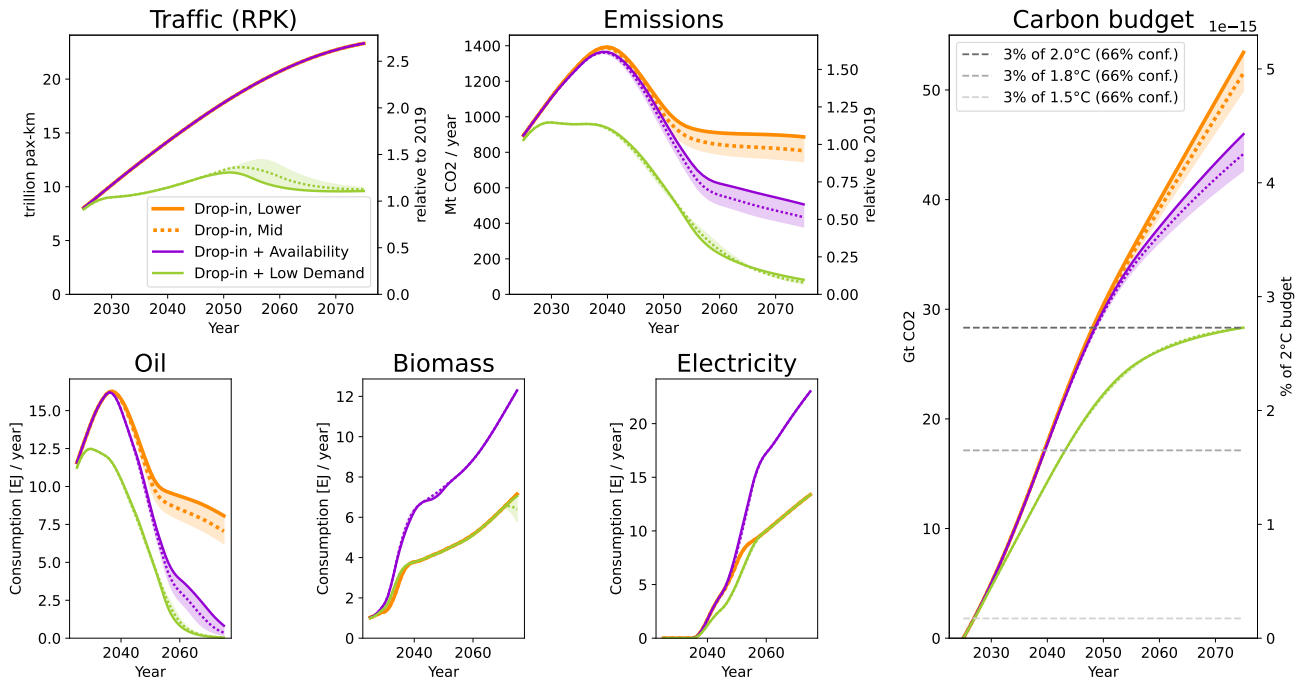


Figure 12: Comparison of drop-in mitigation scenarios under: trend, trend with extra energy availability, and low-demand formulations.

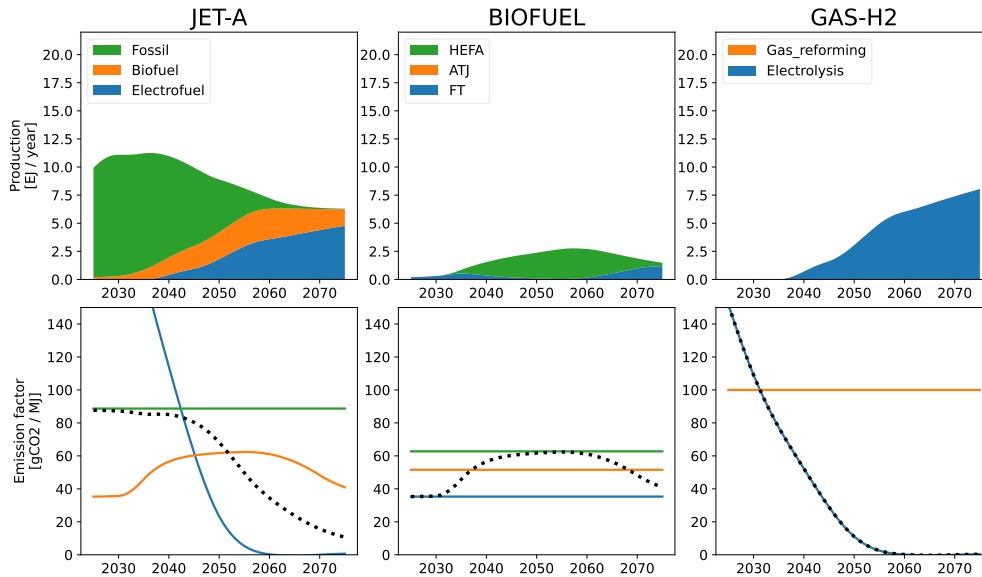


Figure 13: Energy mix and associated carbon intensity under the drop-in mitigation with low-demand formulation and mid aircraft technology. The dotted line represents the mean carbon intensity per energy type.

All simulated scenarios are based on the SSP2-2.6 global scenario. While new aircraft designs can be launched from 2035 to 2060, the fleet simulation spans from 2025 to 2075, this is done to account for the operation and retiring of the current aircraft fleet and also for the delays due to the slow penetration of new designs on the global fleet.

Drop-in mitigation

The scenario outcome with only conventional aircraft is presented in Figure 12.

In the trend scenario, by 2070, emissions reach 762-898 Mt of CO₂ per year, which is comparable to the 2019 emissions of 844.64. Air traffic reaches 22.7 trillion pax-km, representing 2.6 times the 2019 level of 8.7 trillion pax-km. Oil consumption is still 6.8-8.6 EJ per year. Consumption of biomass and electricity reach 6.4 and 12.3 EJ/yr,

Numerical optimization of aviation decarbonization scenarios

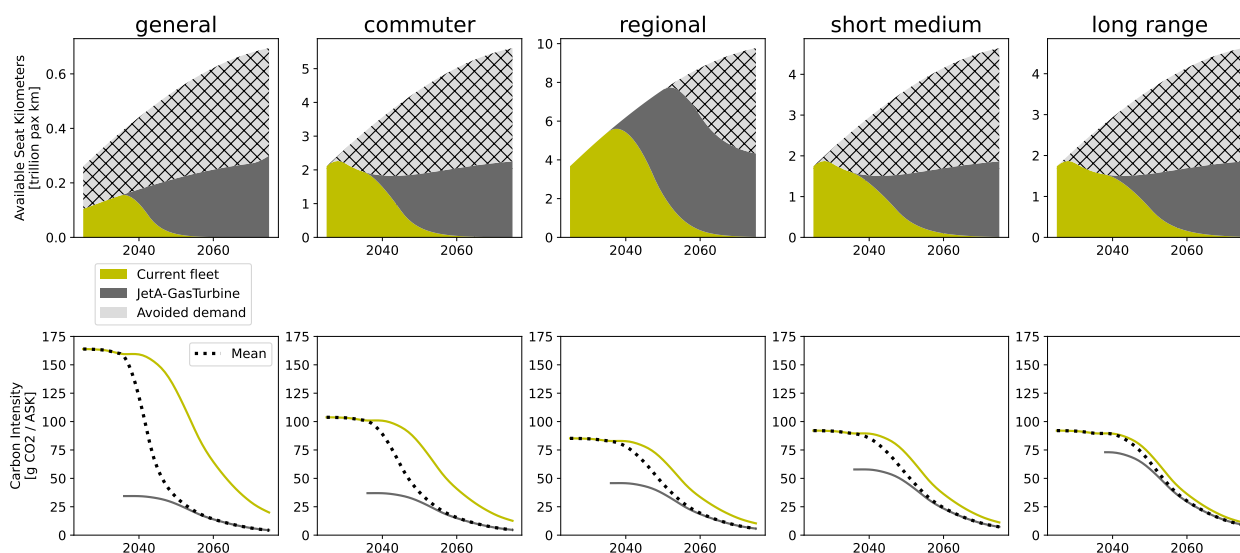


Figure 14: Fleet mix under the drop-in mitigation with low-demand formulation and mid aircraft technology.

respectively. Peak emissions of 1381-1393 Gt/year happens by 2039-2040, and peak oil consumption by 2037 with 16.2-16.3 EJ/yr. Over the 2025 to 2075 period, the sector emitted 49.9-53.4 Gt of CO₂.

In the scenario with extra energy availability, by 2070, emissions reach 415-546 Mt of CO₂ per year, peaking by 2039 with 1357-1366 Mt/yr. Over the 2025 to 2075 period, the sector emitted 42.6-46.0 Gt of CO₂. Oil consumption is 0.5-1.8 EJ per year in 2070, and peaks by 2036 with 16.2 EJ/yr. Consumption of biomass and electricity reach, respectively, 11.0 and 21.2 EJ/yr in 2070. While extra energy availability allows for phasing out of fossil and decreasing emissions in the long run, it is not capable of significantly modifying their peaks.

In the low demand scenario, by 2070, emissions reach 95-114 Mt of CO₂ per year, peaking by 2030 with 968 Mt/yr. Over the 2025 to 2075 period, the sector emitted 28.3 Gt of CO₂. Air traffic reaches 9.6-10.2 trillion pax-km in 2070. Oil consumption is 0.1-0.2 EJ per year in 2070, and peaks by 2030 with 12.5 EJ/yr. Consumption of biomass and electricity reach, respectively, 6.4 and 12.3 EJ/yr in 2070. The presence of traffic aversion makes electricity uptake to happen at a slower pace. Peak oil consumption and emissions happen at lower levels and much sooner than all other scenarios. Because cumulative emissions are constrained, improved technology allows for delaying traffic aversion, which is compensated by more efficient aircraft.

With regards to biofuel pathways, while HEFA displays significantly higher emissions compared to FT, it consumes significantly less biomass. This yields that, in scenarios where fossil kerosene consumption is still high, biomass is preferentially allocated to HEFA production. In Figure 13 one can observe that once fossil kerosene stops being consumed, FT production starts replacing HEFA, which decreases the amount of biofuel production for a given biomass consumption.

Figure 14 details the aircraft mix in the drop-in mitigation with low-demand formulation and upper aircraft technology. Most of the avoided traffic before 2035 come from the general and commuter segments, due to the fact that the 2019 reference fleet has the highest energy consumption per ASK flown. Then, starting in 2030 the short-medium and long-range segments are also avoided due to the energy consumption of the new turbofan designs (see Fig. 11).

Breakthrough mitigation

The scenario outcome with unconventional aircraft is presented in Figure 15. Compared to the scenario with conventional aircraft, scenarios display lower emissions in the trend formulation, and more traffic in the low-demand formulation. Overall, these scenarios also have a wider spread due to the range of technology assumptions, and the lower aircraft technology assumption practically matches emission levels with the drop-in mitigation with upper technology.

Peak oil and peak emissions in the trend scenarios practically match the trend Drop-in mitigation. In the low demand formulation, because more traffic is allowed relative to its Drop-in counterpart, peak oil and emissions happens later, but is more sensitive to technology scenario.

Only the trend scenario with conservative energy allocation has not phased out of oil consumption. The electricity uptake follows a similar pattern to the drop-in mitigation, scenarios with improved aircraft technology have an electricity uptake that is less steep than scenarios with lower technology.

These scenarios also display much lower shares of electrofuel in the Jet-A blend, because hydrogen and electricity are preferentially allocated to alternative aircraft rather than to make electrofuel, but this trade-off is highly dependent on the flight distance considered. Figure 16 shows the energy

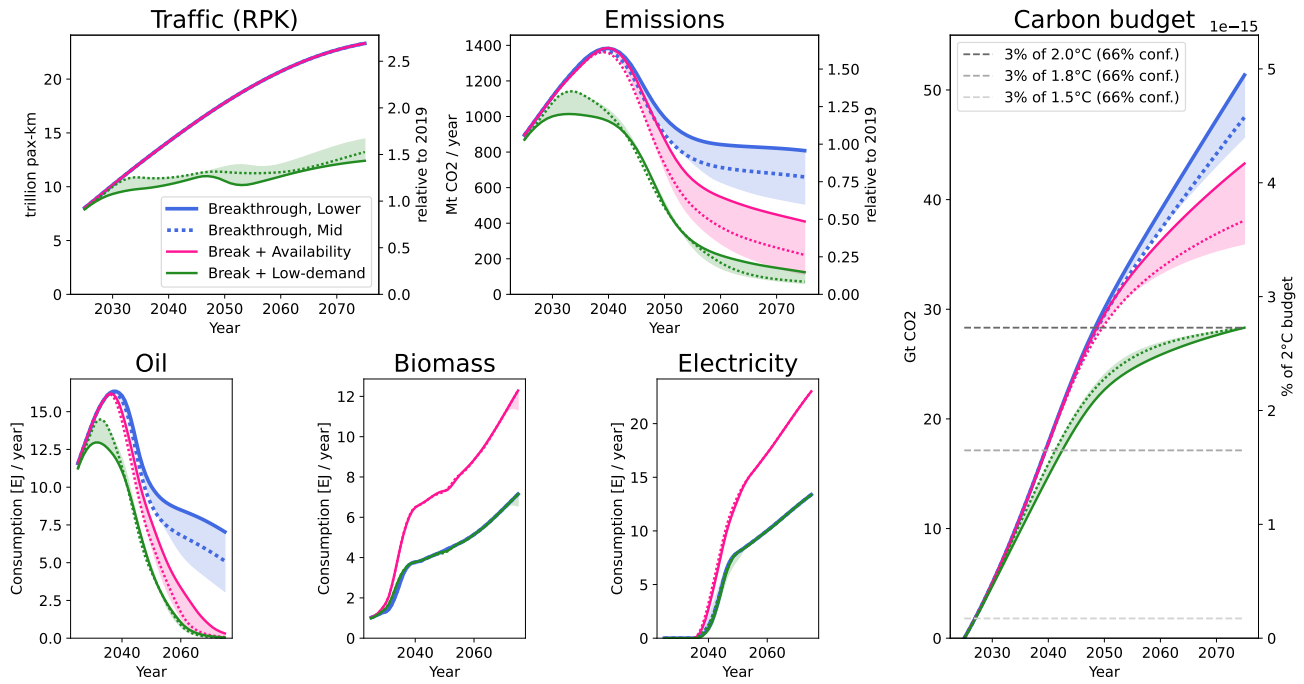


Figure 15: Breakthrough mitigation under: trend, trend with extra energy availability, and low-demand formulations.

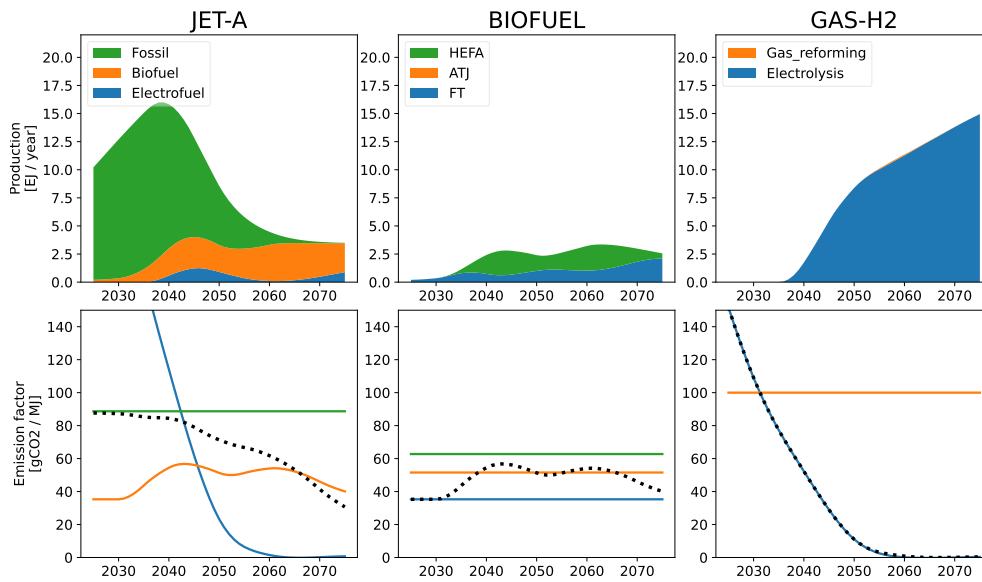


Figure 16: Energy mix under the breakthrough mitigation with trend formulation, extra energy availability, and upper aircraft technology.

mix under an optimistic scenario (for both energy availability and aircraft technology), Figure 17 shows a snapshot of the 2045 energy flows in the same scenario.

In the trend scenario, by 2070, emissions reach 538-822 Mt of CO₂ per year, peaking by 2040 with 1383-1391 Mt/yr. Over the 2025 to 2075 period, the sector emitted 45.7-51.4 Gt of CO₂. Oil consumption is still 3.8-7.6 EJ per year in 2070, and peaks by 2037 with 16.2-16.3 EJ/yr. Consumption of biomass and electricity reach, respectively, 6.4 and 12.3 EJ/yr in 2070.

Figure 18 shows the fleet mix with lower aircraft technology, here hydrogen aircraft with gas turbines are introduced by 2035, and take most of the general and commuter markets, in the regional market hydrogen fuel-cell aircraft is also introduced by 2035, but takes up to 38 % of the market. The rest of the global traffic is supplied by conventional turbofan aircraft introduced by 2035.

With upper aircraft technology (Figure 19). The general market is replaced by electric aircraft by 2037. The commuter market is replaced by hydrogen aircraft with fuel cells

Numerical optimization of aviation decarbonization scenarios

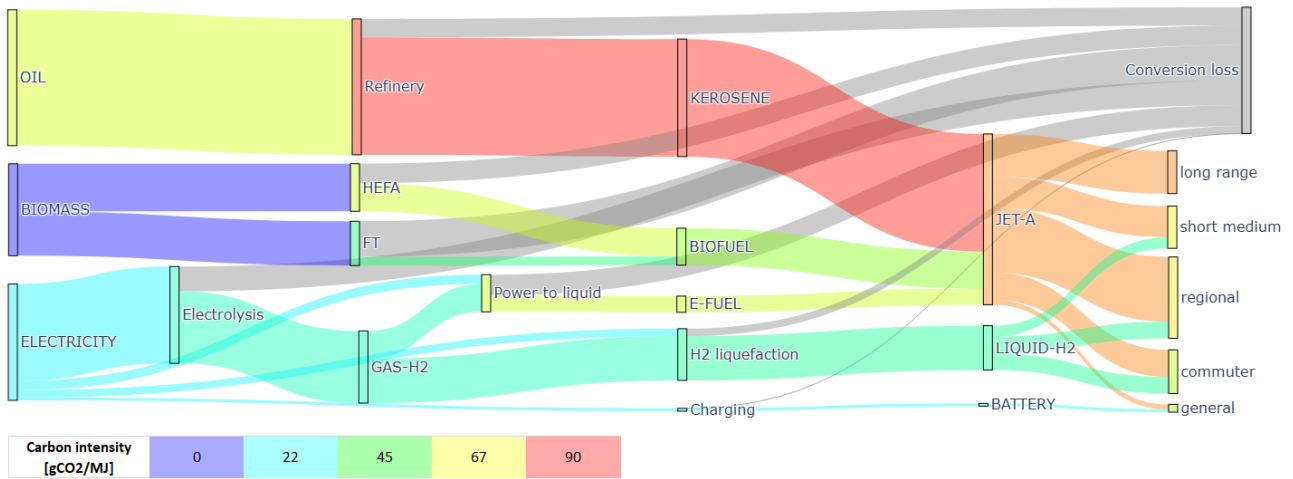


Figure 17: Sankey diagram of energy production for the year 2045 under the breakthrough mitigation with trend formulation, extra energy availability, and upper aircraft technology.

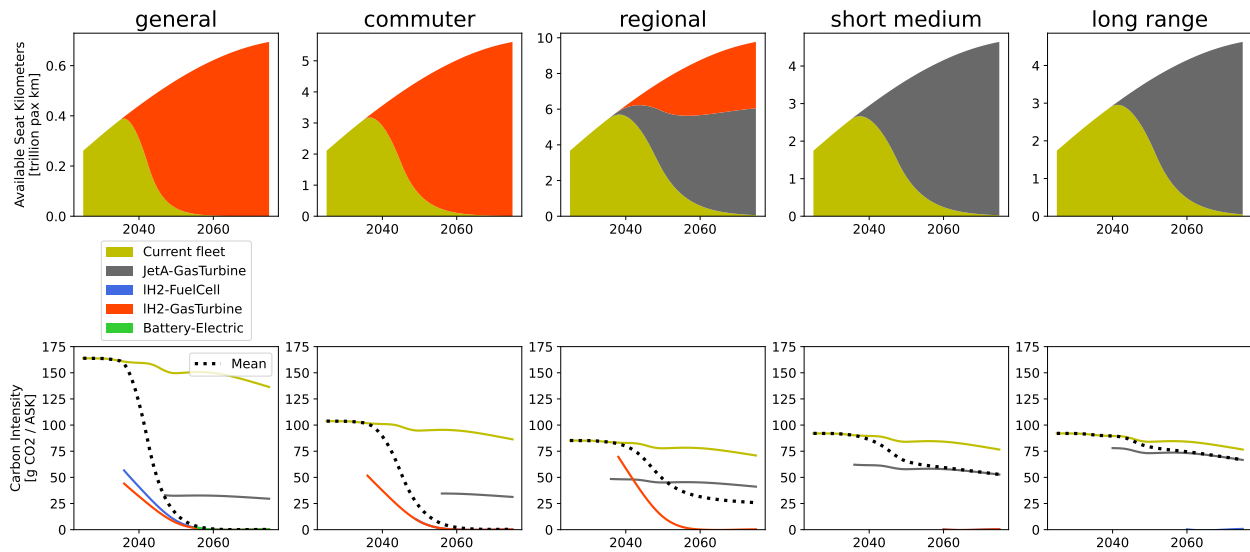


Figure 18: Fleet mix under the breakthrough mitigation with trend formulation and lower aircraft technology.

introduced by 2035. The regional and short-medium markets are introduced to new conventional aircraft by 2035 taking most of both markets. In the regional, however, fuel cell aircraft is also introduced in 2037, taking up to 18 % of the market. The long range is completely replaced by fuel cell aircraft, introduced by 2045. Both Jet-A and hydrogen aircraft display higher energy consumption in the long range, when compared to their short-medium range counterparts (Fig. 11), but introducing hydrogen in the long range, allows for greater decarbonization than in the short-medium despite the increased hydrogen consumption.

In the trend scenario with extra energy availability, by 2070, emissions reach 150-448 Mt of CO₂ per year, peaking by 2039-2040 with 1382-1385 Mt/yr. Over the 2025 to 2075 period, the sector emitted 36.0-43.3 Gt of CO₂. Oil consumption is 0.1-0.8 EJ per year in 2070, and peaks by 2036

with 16.2 EJ/yr. Consumption of biomass and electricity reach, respectively, 11 and 21.2 EJ/yr in 2070.

Figure 20 shows the fleet mix with mid aircraft technology and extra energy availability. Compared to the case with trend availability (Fig. 18), the regional segment is completely replaced by hydrogen aircraft with gas turbines.

In the low-demand scenario, by 2070, emissions reach 76-149 Mt of CO₂ per year, peaking by 2033 with 1014 Mt/yr. Over the 2025 to 2075 period, the sector emitted 28.3 Gt of CO₂. Air traffic reaches 12.1-13.8 trillion pax-km in 2070. Oil consumption is 0.1 EJ per year in 2070, and peaks by 2031-2033 with 13.0-14.5 EJ/yr. Consumption of biomass and electricity reach, respectively, 6.4 and 12.3 EJ/yr in 2070. Electricity consumption reaches similar levels to the trend formulation, but with a slower ramp-up due to lower traffic.

Numerical optimization of aviation decarbonization scenarios

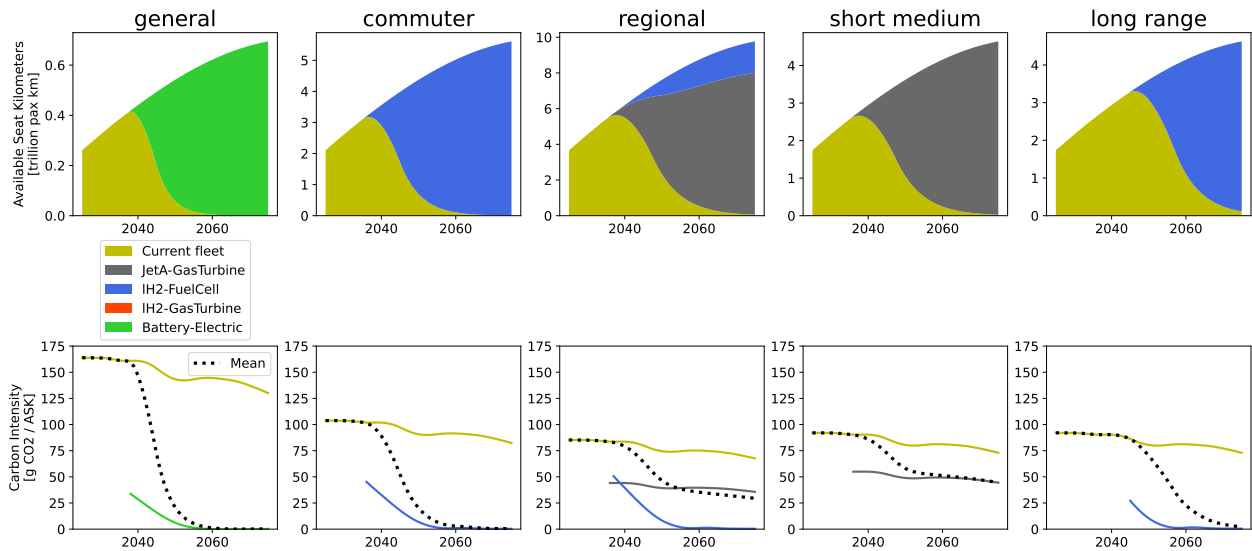


Figure 19: Fleet mix under the breakthrough mitigation with trend formulation and upper aircraft technology.

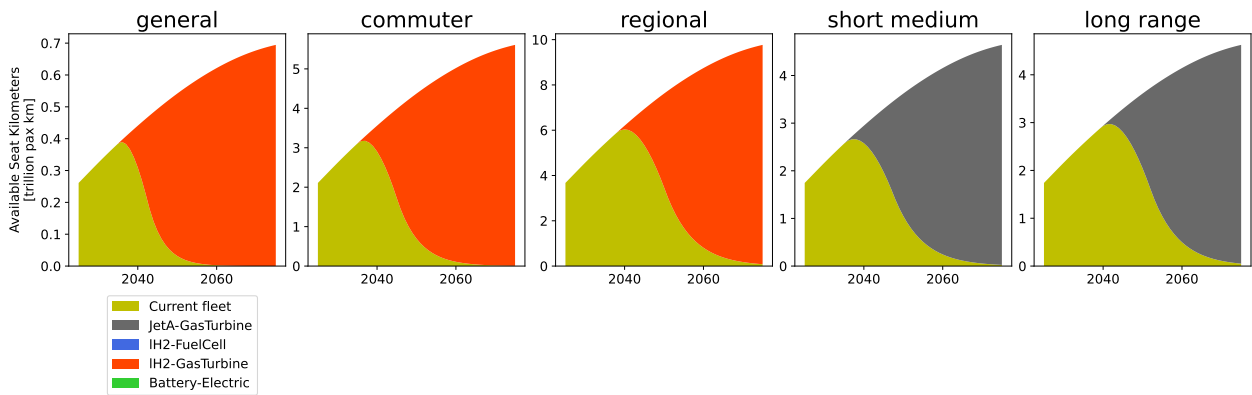


Figure 20: Fleet mix under the breakthrough mitigation with trend formulation with extra energy availability and lower aircraft technology.

Figure 21 details the aircraft mix with low-demand formulation and lower aircraft technology. When compared to the scenario without demand aversion (Fig. 18), the lower demand allows for the entire regional market to be replaced

by hydrogen aircraft. When compared to the drop-in scenario with low demand (Fig. 14), adding unconventional aircraft allows for increasing traffic in the commuter segment after 2050.

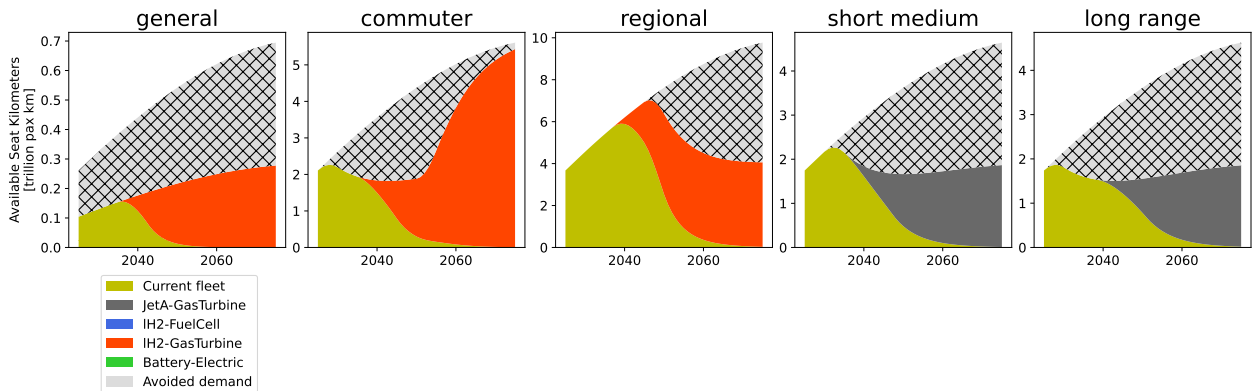


Figure 21: Fleet mix under the breakthrough mitigation with low-demand formulation and lower aircraft technology.

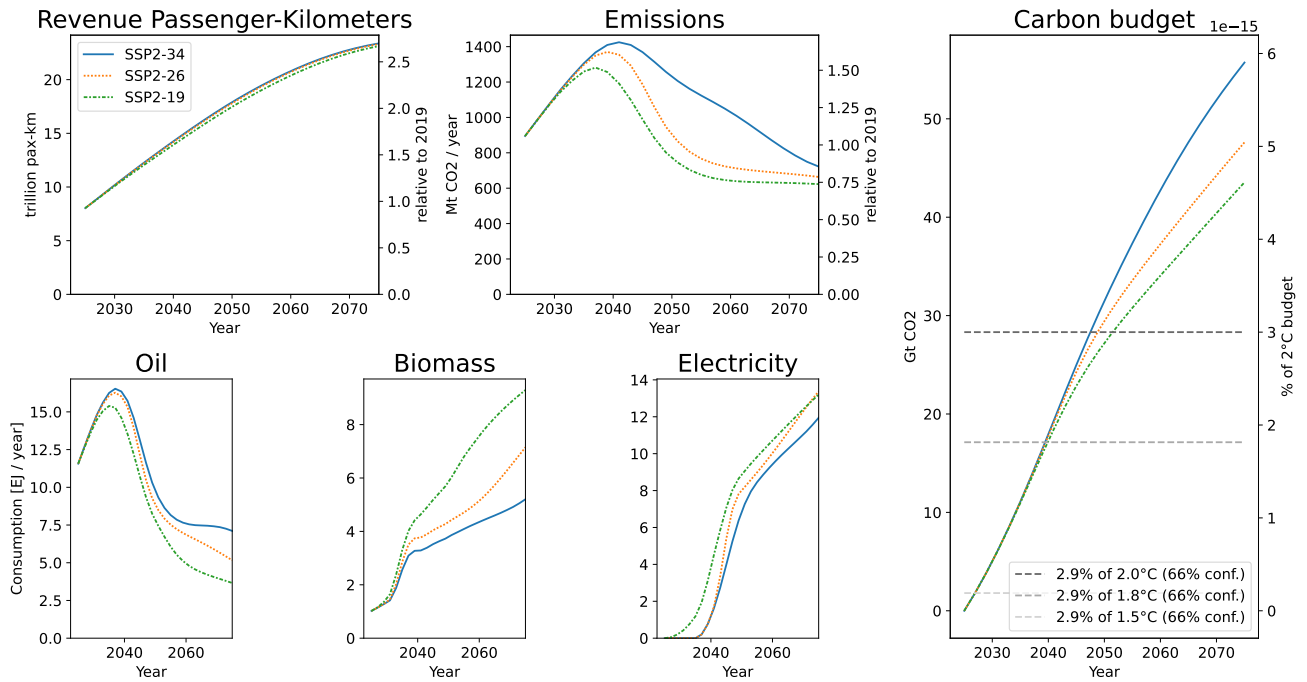


Figure 22: Robust breakthrough mitigation with trend energy availability and SSP2 scenarios with 1.9, 2.6, and 3.4 forcing levels

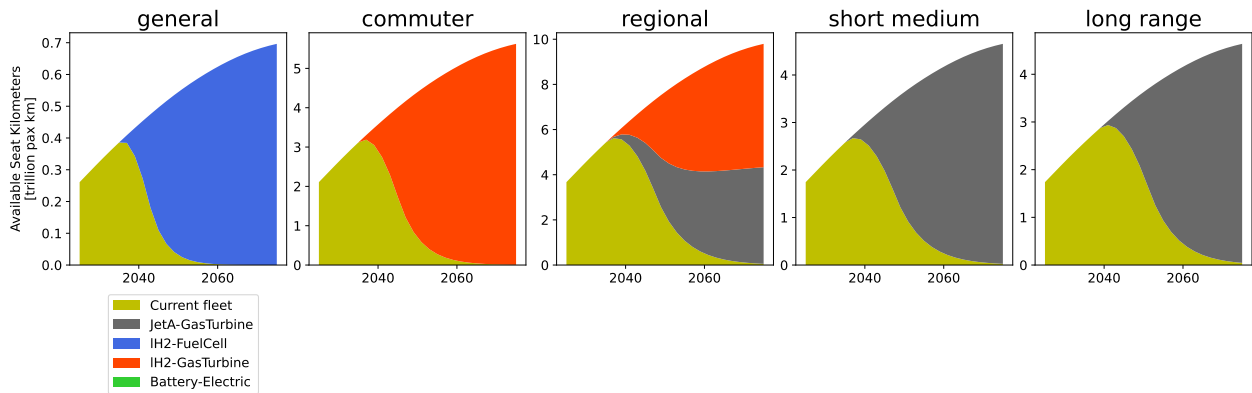


Figure 23: Fleet mix under all scenarios (SSP2 with 1.9, 2.6, and 3.4 forcing levels) within the robust mitigation scenario with trend formulation, conventional energy availability and mid aircraft technology.

4.4. Robustness to background scenario

As the SSP2-2.6 was chosen as background scenario for the single policy optimization, we include scenarios SSP2-1.9 and SSP2-3.4 in the scenario-robust optimization, to account for different radiative forcing targets, representing a more ambitious and a less ambitious scenario. To simplify the analysis, only the trend formulation with conventional energy availability and mid technology is explored.

Figure 22 shows the scenario outcome for the minimization of mean cumulative emissions among all three scenarios. Compared to the single-scenario optimum (Fig. 15), the robust optimum performs slightly worse on the target scenario, yet it allows for greater flexibility in the case an adjacent global happens, instead of the target one.

Figure 23 shows the fleet mix used for all three scenarios. When compared to the single-policy case, smaller shares of alternative aircraft are obtained. This is mainly driven by the strong difference in the availability of electricity and emission factor associated to grid electricity among the scenarios. The overall strategy is to use the worst case scenario (higher electricity emission factor and less electricity availability) to determine the deployment of alternative aircraft, and use the surplus electricity in the other scenarios to make extra electrofuels, leaving room for more variability.

Figures 24, 25, and 26 show the energy mix in the scenarios with 1.9, 2.6, and 3.4 forcing levels, respectively. Among these three scenarios, lower warming levels lead to: earlier deployment of electrofuels due to lower electricity emission factor, higher shares of biofuel in the Jet-A blend

Numerical optimization of aviation decarbonization scenarios

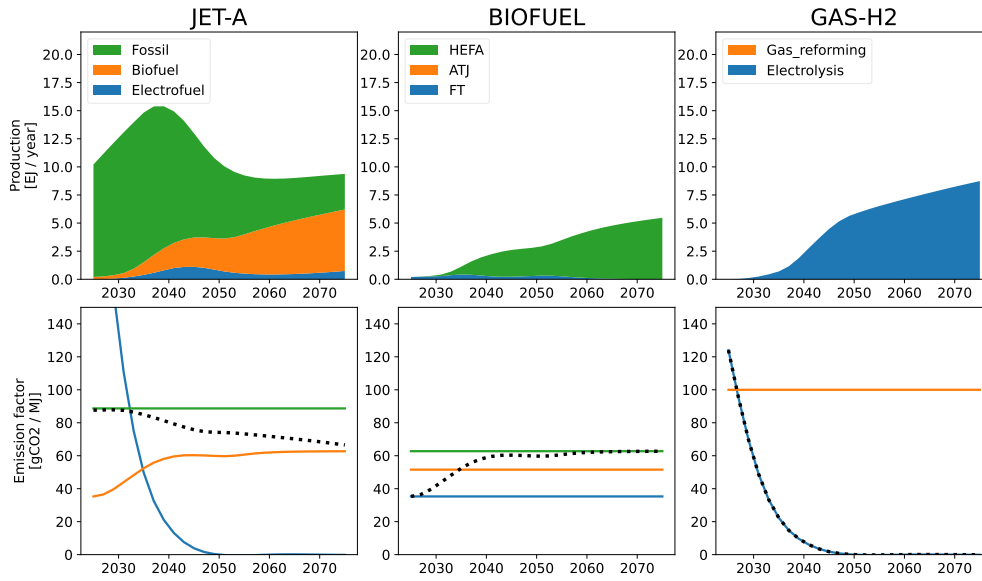


Figure 24: Energy mix under the SSP2-1.9 within the robust mitigation scenario with trend formulation, conventional energy availability and mid aircraft technology.

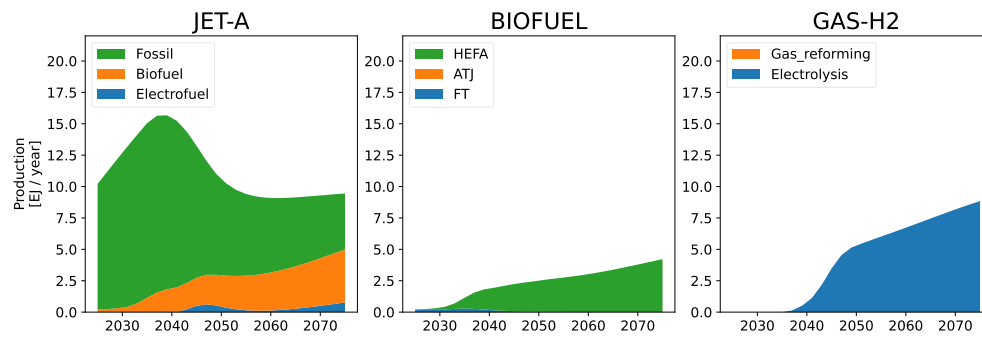


Figure 25: Energy mix under the SSP2-2.6 within the robust mitigation scenario with trend formulation, conventional energy availability and mid aircraft technology.

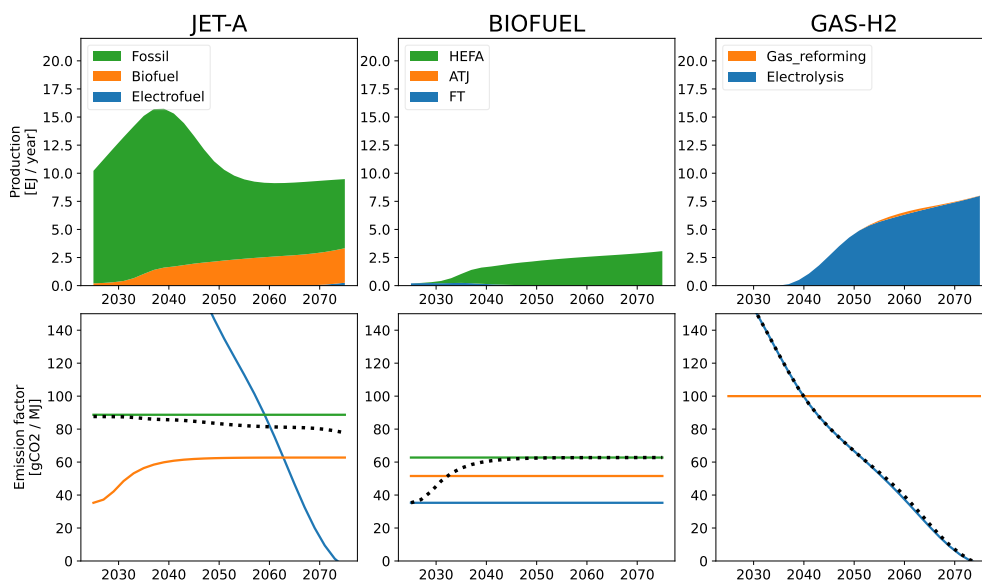


Figure 26: Energy mix under the SSP2-3.4 within the robust mitigation scenario with trend formulation, conventional energy availability and mid aircraft technology.

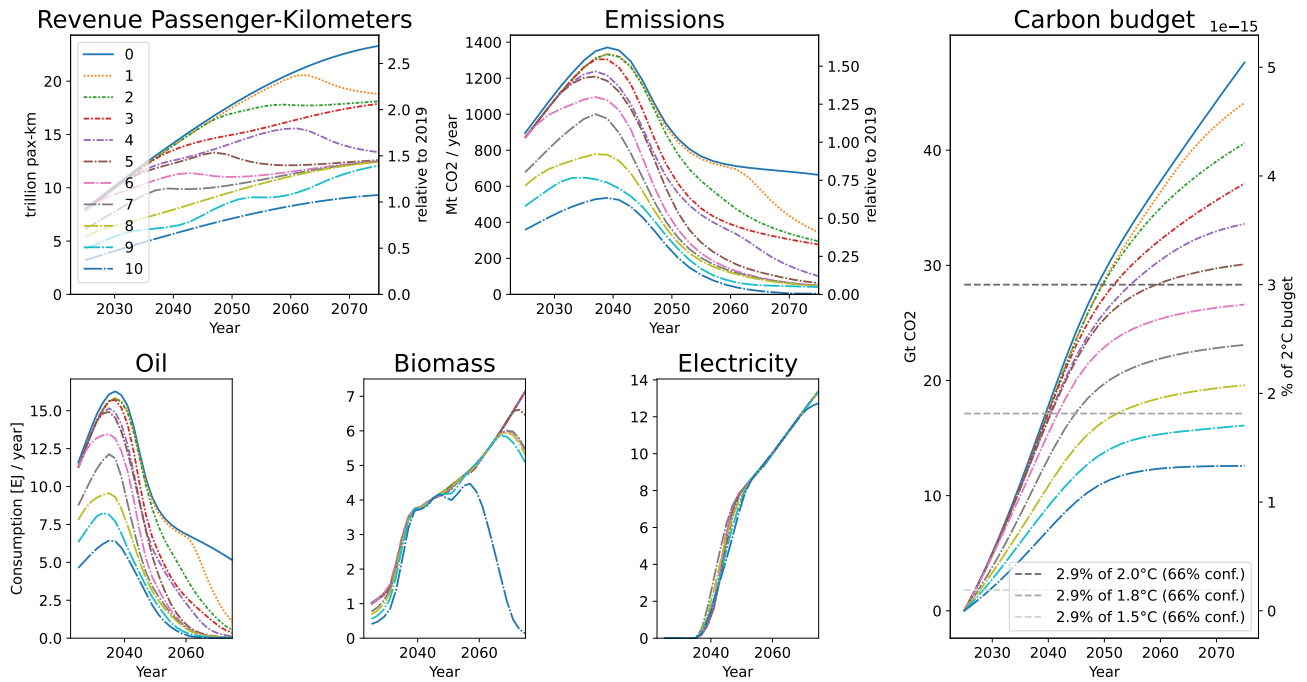


Figure 27: Pareto front scenario comparison with breakthrough mitigation.

due to higher availability of biomass, and higher shares of electrofuel due to the higher electricity availability.

4.5. Traffic and emissions trade-off

The trade-off between the trend and low-demand formulations is performed with resolution of 12 points. Because each formulation has its own objective function, we obtain the Pareto Front solutions of the multiobjective problem to showcase how intermediate scenarios can be obtained from each of the single-objective optima.

To simplify the analysis of traffic and emissions trade-off, only the mid aircraft technology was considered for drop-in and breakthrough mitigation, both with conservative and preferential energy availability.

Figure 27 shows the scenario outcome of each point in the Pareto Front of the Breakthrough mitigation with conventional energy availability. Scenario 0 corresponds to the upper right-most point in the Pareto Front (all trend demand is met), from that point onwards the carbon budget constraint decreases until reaching its value with maximal demand avoidance.

From scenarios 0 to 5, most of the demand and emissions reduction is achieved by constraining post-2040 traffic, specially in the most carbon-intense markets. This is expected as the objective function (Eq. 7) has a discount factor, which decreases the valuation of demand reductions happening in the far future. After this point, of around 3.0 % of the carbon budget for 2°C, achieving stricter mitigation targets requires reducing demand at earlier moments in time, while leaving traffic volumes post-2060 at similar levels, of nearly 150 % of 2019's traffic by 2075. This happens because after 2060 electricity is practically net-zero emissions (Fig. 9, so all the

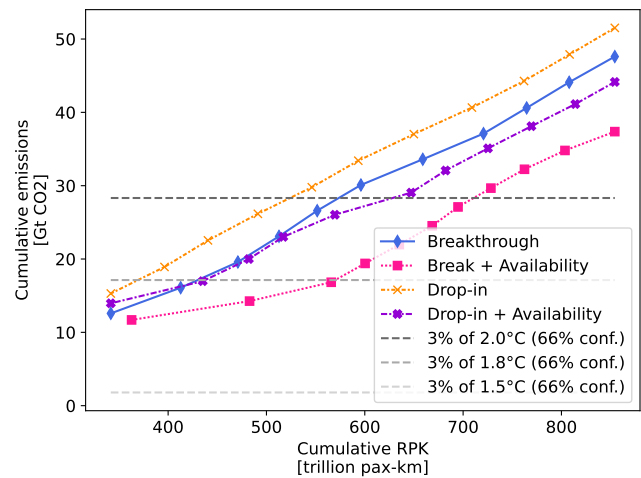


Figure 28: Pareto Front of traffic and cumulative emissions.

flights that operate with batteries, hydrogen, or electrofuel are still allowed to operate.

In Figure 28 the traffic and emissions Pareto Front is shown, each point representing the result of an individual sub-optimization that was carried for the multi-objective problem.

Considering scenarios that do not respect the 2°C budget, trends are similar to the results found in the single-scenario optimization: energy availability alone is more effective at reducing emissions (or increasing traffic) than introduction of unconventional aircraft alone, here one can also observe that their combined effect is capable of reaching even lower emissions. But considering stricter emission caps

and lower traffic levels (near the 1.8°C budget), reverts this behavior and yields that unconventional aircraft alone can become more effective than energy availability alone.

For the scenario with unconventional aircraft and extra energy availability, there is even a significant margin, from the lowest admissible traffic, for demand to grow without extra cumulative emissions (net-zero). From that point, every increase in traffic will lead to more cumulative emissions (similar to other scenarios).

5. Limitations

This section describes the limitations of the numerical methods and the simplifying hypothesis made by the models used in the present paper.

Firstly, using differential programming paradigms requires implementing model equations in specific frameworks, which may be stricter than original implementations that don't allow for AD. While the results themselves are not affected, the limitation here is related to rethinking parts of implementation, especially for conditional statements, iterative processes, and in-place replacement.

Secondly, the limitations of the models are noted for each elementary model:

Air traffic demand

The use of logistic equations, when compared to constant elasticity models, allows for better account of the economic development of countries, but using these in a forward-looking manner means exploiting the model outside of its calibrated range, which can be particularly problematic when estimating saturation levels in countries that have not yet reached the inflection point of the curve.

The scenarios here are aggregated on a global level, which does not account for regional disparities in demand growth, carbon content of electricity, and biomass availability.

Also, even though mitigation costs are not modeled in this work, prices are also a driver for demand modifications through price elasticity. Implementing this effect leads to a coupled system (energy cost depends on traffic volumes, which depends on ticket prices), which is highly dependent on policy, e.g., taxes and incentives.

Aircraft design

TLAR are kept the same for each architecture within a market, but aircraft size, speed, and altitude can have affect vehicle performance and ideally should be optimized for each of them.

Cryogenic tank gravimetric efficiency matures with time, but is kept fixed among markets. This ignores dependency on tank size [11, 48], the upper technology scenario may figure values that are not realistic for small aircraft.

Finally, gas turbine performance weight and consumption was kept the same between kerosene and hydrogen. Literature shows that energy consumption may be slightly different when burning hydrogen [85], but few information is available on the weight penalty of such engines.

Fleet deployment

Within each market segment, aircraft architectures are tailored for the flown distances. Yet, in practice airlines may operate aircraft over distances that are different from which the aircraft was optimized for, this leads to increased fuel consumption in reality and explains the lower historical efficiencies for the general and commuter segments.

Energy-mix

Because the energy production models are formulated to be "controlled" by the optimizer using a time-delay on the shares of production (rather than production volumes itself), whenever production volumes of energy carriers varyies rapidly, the pathway production struggles to adapt its shares to keep steady production levels. For example, around 2050 in scenarios with introduction of alternative aircraft, the consumption of Jet-A decreases sharply leading to some oscillations in the total biomass consumption and in the repartition of biofuel production among the modeled pathways.

No difference is made between biomass types, which means all pathways compete for the same resource. In practice, each biofuel pathway consume specific feedstocks that may not necessarily compete with each-other and subject to very different production volumes.

Finally, the electricity consumption associated with the power-to-liquid pathway (Tab. 4) is representative of a process that uses solely Direct Air Capture as the CO₂ source. Using concentrated CO₂ sources can significantly decrease this and while some assessments conclude that some regional sources are sufficient to ramp-up production [86], the assumption of no competition for the CO₂ volumes can be highly questionable, especially when accounting other transportation modes.

6. Discussion

Considering trend traffic growth and allocation of energy resources, even with optimistic technological breakthrough, aviation share of emissions will grow as the wider economy decarbonizes in a 2°C temperature increase scenario. This is in line with scenarios from the IPCC's 6th Assessment Report [87, Figure 3.19], in which transport emissions take the longest to reach net zero even in scenarios below 1.5°C with little overshoot.

Regarding the implications for the energy system, fulfilling aviation's needs will require significant volumes of low-carbon electricity and biomass. Limited production amounts will require dedicated policy on which sectors to prioritize the access to these resources. These findings are also in line with recent studies focused on the aviation sector [1, 16, 86]. Dedicated production facilities integrated near airports might be a way to reducing associated supply chain losses and costs [17].

As the efficiencies of energy conversion processes can vary strongly depending on the primary energy source, their comparison must be made on a per unit of service basis. While some studies on several transport modes [45] consider

the base service unit as 1 MJ of thrust (or to wheels), this work instead, considers it to be a traffic measure (passenger-kilometer). This distinction is fundamental for aviation due to the different weights of the propulsion architectures to power these vehicles. For example, a heavier propulsion system (such as current battery and cryogenic tank technology) would require more thrust to transport the same payload over a given distance.

Air transportation is highly unequal sector, both across (Fig. 3) and within [88] countries. Given that most of the traffic growth in the next decades will happen in emerging economies, which have not yet reached demand saturation. Many of these, however, are still steering public policy to increase access to air travel, e.g., [89]. The public acceptance and effectiveness of demand-side measures can be questioned, and using pricing mechanisms to address this problem also raises questions of social justice [90].

Also, climate change is but one within the Planetary Boundaries [91, 92]. Some recent assessments that expand the scope for other Planetary Boundaries [72] stress on the need for acknowledging other limits to avoid shifting the problem, such as biodiversity loss and eutrophication of freshwater ecosystems, especially when considering a strong uptake of biofuels, which are present in most of the industry decarbonization roadmaps [1].

Given a set of technology forecasts, optimization can be useful for deciding which technologies to prioritize and when, especially when they compete for similar resources. Yet, in many IAM applications that use optimization, the formulation of the optimization problem is often left unchanged or is little discussed, even if the choice of policy goal (objective) and non-negotiables (constraints) are a fundamental part of the process.

7. Conclusion

The use of GEMSEO-JAX allowed for both reducing implementation burden and execution time for the optimization of mitigation scenarios. Achieved speedups are of two and three orders of magnitude, respectively, at the scenario optimization level, and at the scenario computation and linearization level.

The choice of which aircraft architecture and energy carrier to embark is highly dependent on vehicle performance (determined by TLAR and technology assumptions) and on the background energy system (due to the timing of electricity decarbonization and to limited availability of electricity and biomass).

In order to respect Paris Agreement targets under an effort-sharing principle, drop-in mitigation will put the system to a higher stress: either by constraining traffic, or by consuming too much biomass and electricity. New aircraft with alternative energy carriers allows to reduce such stress by making better use of the same energy resources, even if their energy consumption is higher than that of conventional planes.

When comparing mitigation policies with different objective functions, namely traffic and emissions trade-off, it was found that supply caps, energy availability, and the introduction of alternative aircraft designs are complementary rather than competing measures. One strategy alone can achieve reduction in emissions up to a certain level, but their combined use is capable of more efficient mitigation by: using alternative aircraft in its feasible markets (reducing needs for low-carbon electricity and biomass for a given service), and avoiding emission-intense markets (further reducing consumption of fossil kerosene).

Our research offers practical insights on how to efficiently use optimization algorithms for mitigation scenarios. Applying these methods for the aviation sector, also shed light on how to optimally allocate aircraft architectures, energy resources, and demand-side measures to achieve stringent mitigation targets.

Code availability

All the scripts and data required to reproduce the results from this work are openly available in <https://gitlab.com/ian.costa-alves1/noads>.

Acknowledgements

Gratitude is extended to the Conceptual Airplane Design and Operations (CADO) team at École Nationale de l'Aviation Civile (ENAC), to the Aviation, Climate, Environment (ACE) group at ISAE-SUPAERO, and to the Institute for Sustainable Aviation (ISA) for their support, assistance, and fruitful discussions. The Generic Aircraft Design Model (GAM), provided by the CADO team, was essential for enabling modeling and analysis of alternative aircraft designs. The AeroMAPS platform, developed by ISAE-SUPAERO and ISA, was responsible for laying the groundwork upon which this research was built, when the methodology was first introduced many models were a direct re-implementation of AeroMAPS equations, currently this is still true for the the load factor (Eq. 5) model. Special thanks to Pascal Roches, Nicolas Monrolin, Thomas Planès, Scott Delbecq, Antoine Salgas, Florian Simatos, Laurent Joly, and Xavier Carbonneau for their sharp insights, support, and collaboration.

Also, the authors thank the Multidisciplinary Optimization Competence Center at IRT Saint Exupéry, for their availability and support with the methodological developments that preceded this research. Special thanks to Matthias De Lozzo, and Antoine Dechaume for their aid with repository maintenance and thorough code reviews.

CRedit authorship contribution statement

Ian Costa-Alves: Writing – original draft, Writing – review & editing, Conceptualization, Data curation, Investigation, Methodology, Software, Validation, Visualization.

Nicolas Gourdain: Writing – original draft, Writing – review & editing, Conceptualization, Methodology, Funding acquisition, Project administration, Supervision.

François Gallard: Writing – original draft, Writing – review & editing, Conceptualization, Methodology, Software, Supervision.

Anne Gazaix: Writing – review & editing, Conceptualization, Funding acquisition, Project administration, Supervision.

Yri Amandine Kambiri: Writing – review & editing, Software, Validation.

Thierry Druot: Writing – review & editing, Conceptualization, Software, Supervision, Validation.

Funding sources

This work was supported by the Occitania region, ISAE-SUPAERO, and IRT Saint Exupéry.

References

- [1] S. Becken, B. Mackey, D. S. Lee, Implications of preferential access to land and clean energy for Sustainable Aviation Fuels, *Science of The Total Environment* 886 (2023) 163883. doi:10.1016/j.scitotenv.2023.163883.
URL <https://linkinghub.elsevier.com/retrieve/pii/S0048969723025044>
- [2] B. Girod, D. P. van Vuuren, S. Deetman, Global travel within the 2 °C climate target, *Energy Policy* 45 (2012) 152–166. doi:10.1016/j.enpol.2012.02.008.
URL <https://www.sciencedirect.com/science/article/pii/S0301421512001127>
- [3] P. J. Ansell, Review of sustainable energy carriers for aviation: Benefits, challenges, and future viability, *Progress in Aerospace Sciences* 141 (2023) 100919. doi:10.1016/j.paerosci.2023.100919.
URL <https://linkinghub.elsevier.com/retrieve/pii/S0376042123000350>
- [4] R. S. Märkl, C. Voigt, D. Sauer, R. K. Dischl, S. Kaufmann, T. Harlaß, V. Hahn, A. Rojger, C. Weiß-Rehm, U. Burkhardt, U. Schumann, A. Marsing, M. Scheibe, A. Dörnbrack, C. Renard, M. Gauthier, P. Swann, P. Madden, D. Luff, R. Sallinen, T. Schripp, P. Le Clercq, Powering aircraft with 100 % sustainable aviation fuel reduces ice crystals in contrails, *Atmospheric Chemistry and Physics* 24 (6) (2024) 3813–3837. doi:10.5194/acp-24-3813-2024.
URL <https://acp.copernicus.org/articles/24/3813/2024/>
- [5] D. Raymer, *Aircraft Design: A Conceptual Approach*, Sixth Edition, American Institute of Aeronautics and Astronautics, Inc., Washington, DC, 2018. doi:10.2514/4.104909.
URL <https://arc.aiaa.org/doi/book/10.2514/4.104909>
- [6] P. Jaramillo, S. K. Ribeiro, P. Newman, S. Dhar, O. Diemuodeke, T. Kajino, D. Lee, S. Nugroho, X. Ou, A. H. Strømman, J. Whitehead, Transport, in: *Intergovernmental Panel On Climate Change (IPCC) (Ed.), Climate Change 2022 - Mitigation of Climate Change*, 1st Edition, Cambridge University Press, 2023, Ch. 10, pp. 1049–1160. doi:10.1017/9781009157926.012.
URL https://www.cambridge.org/core/product/identifier/9781009157926%23c10/type/book_part
- [7] K. Riahi, D. P. van Vuuren, E. Kriegler, J. Edmonds, B. C. O'Neill, S. Fujimori, N. Bauer, K. Calvin, R. Dellink, O. Fricko, W. Lutz, A. Popp, J. C. Cuaresma, S. Kc, M. Leimbach, L. Jiang, T. Kram, S. Rao, J. Emmerling, K. Ebi, T. Hasegawa, P. Havlik, F. Humpenöder, L. A. Da Silva, S. Smith, E. Stehfest, V. Bosetti, J. Eom, D. Gernaat, T. Masui, J. Rogelj, J. Strefler, L. Drouet, V. Krey, G. Luderer, M. Harmsen, K. Takahashi, L. Baumstark, J. C. Doelman, M. Kainuma, Z. Klimont, G. Marangoni, H. Lotze-Campen, M. Obersteiner, A. Tabeau, M. Tavoni, The Shared Socioeconomic Pathways and their energy, land use, and greenhouse gas emissions implications: An overview, *Global Environmental Change* 42 (2017) 153–168. doi:10.1016/j.gloenvcha.2016.05.009.
URL <https://www.sciencedirect.com/science/article/pii/S0959378016300681>
- [8] M. Sharmina, O. Y. Edelenbosch, C. Wilson, R. Freeman, D. E. H. J. Gernaat, P. Gilbert, A. Larkin, E. W. Littleton, M. Traut, D. P. van Vuuren, N. E. Vaughan, F. R. Wood, C. Le Quéré, Decarbonising the critical sectors of aviation, shipping, road freight and industry to limit warming to 1.5–2°C, *Climate Policy* 21 (4) (2021) 455–474, publisher: Taylor & Francis_eprint: <https://doi.org/10.1080/14693062.2020.1831430>. doi:10.1080/14693062.2020.1831430.
URL <https://doi.org/10.1080/14693062.2020.1831430>
- [9] T. A. Napp, S. Few, A. Sood, D. Bernie, A. Hawkes, A. Gambhir, The role of advanced demand-sector technologies and energy demand reduction in achieving ambitious carbon budgets, *Applied Energy* 238 (2019) 351–367. doi:10.1016/j.apenergy.2019.01.033.
URL <https://www.sciencedirect.com/science/article/pii/S0306261919300339>
- [10] S. Speizer, J. Fuhrman, L. Aldrete Lopez, M. George, P. Kyle, S. Monteith, H. McJeon, Integrated assessment modeling of a zero-emissions global transportation sector, *Nature Communications* 15 (1) (2024) 4439, publisher: Nature Publishing Group. doi:10.1038/s41467-024-48424-9.
URL <https://www.nature.com/articles/s41467-024-48424-9>
- [11] E. J. Adler, J. R. Martins, Hydrogen-powered aircraft: Fundamental concepts, key technologies, and environmental impacts, *Progress in Aerospace Sciences* 141 (2023) 100922. doi:10.1016/j.paerosci.2023.100922.
URL <https://linkinghub.elsevier.com/retrieve/pii/S0376042123000386>
- [12] J. Mukhopadhaya, D. Rutherford, Performance analysis of evolutionary hydrogen-powered aircraft (Jan. 2022).
URL <https://theicct.org/publication/aviation-global-evo-hydrogen-aircraft-jan22/>
- [13] J. Mukhopadhaya, Performance Analysis of Fuel Cell Retrofit Aircraft (Aug. 2023).
URL <https://theicct.org/publication/fuel-cell-retrofit-aug23/>
- [14] J. Mukhopadhaya, B. Graver, Performance analysis of regional electric aircraft (Jul. 2022).
URL <https://theicct.org/publication/global-aviation-performance-analysis-regional-electric-aircraft-jul22/>
- [15] V. Grewe, A. Gangoli Rao, T. Grönstedt, C. Xisto, F. Linke, J. Melkert, J. Middel, B. Ohlenforst, S. Blakey, S. Christie, S. Matthes, K. Dahlmann, Evaluating the climate impact of aviation emission scenarios towards the Paris agreement including COVID-19 effects, *Nature Communications* 12 (1) (2021) 3841. doi:10.1038/s41467-021-24091-y.
URL <https://www.nature.com/articles/s41467-021-24091-y>
- [16] J. Eaton, M. Naraghi, J. G. Boyd, Regional pathways for all-electric aircraft to reduce aviation sector greenhouse gas emissions, *Applied Energy* 373 (2024) 123831. doi:10.1016/j.apenergy.2024.123831.
URL <https://linkinghub.elsevier.com/retrieve/pii/S0306261924012145>
- [17] J. Hoelzen, D. Silberhorn, F. Schenke, E. Stabenow, T. Zill, A. Bensmann, R. Hanke-Rauschenbach, H₂-powered aviation – Optimized aircraft and green LH₂ supply in air transport networks, *Applied Energy* 380 (2025) 124999. doi:10.1016/j.apenergy.2024.124999.
URL <https://linkinghub.elsevier.com/retrieve/pii/S0306261924023833>
- [18] S. Delbecq, J. Fontane, N. Gourdain, T. Planès, F. Simatos, Sustainable aviation in the context of the Paris Agreement: A review of prospective scenarios and their technological mitigation levers, *Progress in Aerospace Sciences* 141 (2023) 100920. doi:10.1016/j.paerosci.2023.100920.
URL <https://linkinghub.elsevier.com/retrieve/pii/S0376042123000362>

- [19] T. Planès, S. Delbecq, A. Salgas, AeroMAPS: a framework for performing multidisciplinary assessment of prospective scenarios for air transport, *Journal of Open Aviation Science* 1 (1) (Dec. 2023). doi:10.59490/joas.2023.7147.
URL <https://journals.open.tudelft.nl/joas/article/view/7147>
- [20] E. Byers, V. Krey, E. Krieglner, K. Riahi, R. Schaeffer, J. Kikstra, R. Lamboll, Z. Nicholls, M. Sandstad, C. Smith, K. van der Wijst, A. Al Khouradje, F. Lecocq, J. Portugal-Pereira, Y. Saheb, A. Stromann, H. Winkler, C. Auer, E. Brutschin, M. Gidden, P. Hackstock, M. Harmsen, D. Huppmann, P. Kolp, C. Lepault, J. Lewis, G. Marangoni, E. Müller-Casseres, R. Skeie, M. Werning, K. Calvin, P. Forster, C. Guivarch, T. Hasegawa, M. Meinshausen, G. Peters, J. Rogelj, B. Samset, J. Steinberger, M. Tavoni, D. van Vuuren, Ar6 scenarios database (Nov. 2022). doi:10.5281/zenodo.5886911.
URL <https://doi.org/10.5281/zenodo.5886911>
- [21] I. Costa-Alves, N. Gourdain, F. Gallard, A. Gazaix, Optimal aircraft fleet and energy mix under limited availability of resources, in: 26th Conference of the International Society for Air Breathing Engines, International Society for Air Breathing Engines (ISABE), Toulouse, France, 2024.
URL <https://hal.science/hal-04735803>
- [22] D. Lee, D. Fahey, A. Skowron, M. Allen, U. Burkhardt, Q. Chen, S. Doherty, S. Freeman, P. Forster, J. Fuglestedt, A. Gettelman, R. De León, L. Lim, M. Lund, R. Millar, B. Owen, J. Penner, G. Pitari, M. Prather, R. Sausen, L. Wilcox, The contribution of global aviation to anthropogenic climate forcing for 2000 to 2018, *Atmospheric Environment* 244 (2021) 117834. doi:10.1016/j.atmosenv.2020.117834.
URL <https://linkinghub.elsevier.com/retrieve/pii/S1352231020305689>
- [23] L. Megill, K. Deck, V. Grewe, Alternative climate metrics to the Global Warming Potential are more suitable for assessing aviation non-CO2 effects, *Communications Earth & Environment* 5 (1) (2024) 249. doi:10.1038/s43247-024-01423-6.
URL <https://www.nature.com/articles/s43247-024-01423-6>
- [24] P. Proesmans, Climate-optimal aircraft design and fleet allocation: Evaluating the impact of sustainable aviation fuels, Ph.D. thesis, Delft University of Technology (2024).
URL <https://resolver.tudelft.nl/uuid:295a037d-02ef-4bb9-bd4e-c6e346f0fefa>
- [25] W. D. Nordhaus, An Optimal Transition Path for Controlling Greenhouse Gases, *Science* 258 (5086) (1992) 1315–1319. doi:10.1126/science.258.5086.1315.
URL <https://www.science.org/doi/10.1126/science.258.5086.1315>
- [26] L. Barrage, W. Nordhaus, Policies, Projections, and the Social Cost of Carbon: Results from the DICE-2023 Model, Tech. Rep. w31112, National Bureau of Economic Research, Cambridge, MA (Apr. 2023). doi:10.3386/w31112.
URL <http://www.nber.org/papers/w31112.pdf>
- [27] K. Calvin, P. Patel, L. Clarke, G. Asrar, B. Bond-Lamberty, R. Y. Cui, A. Di Vittorio, K. Dorheim, J. Edmonds, C. Hartin, M. Hejazi, R. Horowitz, G. Iyer, P. Kyle, S. Kim, R. Link, H. McJeon, S. J. Smith, A. Snyder, S. Waldhoff, M. Wise, Gcam v5.1: representing the linkages between energy, water, land, climate, and economic systems, *Geoscientific Model Development* 12 (2) (2019) 677–698. doi:10.5194/gmd-12-677-2019.
URL <https://gmd.copernicus.org/articles/12/677/2019/>
- [28] OS-Climate, WITNESS Overview.
URL <https://www.witness4climate.org/witness-overview-3/>
- [29] D. Huppmann, M. Gidden, O. Fricko, P. Kolp, C. Orthofer, M. Pimmer, N. Kushin, A. Vinca, A. Mastrucci, K. Riahi, V. Krey, The MESSAGEix Integrated Assessment Model and the *ix modeling platform* (ixmp): An open framework for integrated and cross-cutting analysis of energy, climate, the environment, and sustainable development, *Environmental Modelling & Software* 112 (2019) 143–156. doi:10.1016/j.envsoft.2018.11.012.
URL <https://www.sciencedirect.com/science/article/pii/S1364815218302330>
- [30] J. G. C. R. Institute, Cassandra model coupling framework, original-date: 2014-12-04T15:48:06Z (Nov. 2024).
URL <https://github.com/JGCRI/cassandra>
- [31] A. Salgas, T. Planès, S. Delbecq, F. Simatos, G. Lafforgue, Cost estimation of the use of low-carbon fuels in prospective scenarios for air transport, in: AIAA SCITECH 2023 Forum, American Institute of Aeronautics and Astronautics, National Harbor, MD & Online, 2023. doi:10.2514/6.2023-2328.
URL <https://arc.aiaa.org/doi/10.2514/6.2023-2328>
- [32] A. Salgas, G. Lafforgue, T. Planès, S. Delbecq, Marginal Abatement Cost Curves for Aviation: Metrics and Prospective Decarbonisation Scenarios Analysis (2024). doi:10.2139/ssrn.4853510.
URL <https://www.ssrn.com/abstract=4853510>
- [33] L. Dray, A. W. Schäfer, C. Grobler, C. Falter, F. Allroggen, M. E. J. Stettler, S. R. H. Barrett, Cost and emissions pathways towards net-zero climate impacts in aviation, *Nature Climate Change* 12 (10) (2022) 956–962, publisher: Nature Publishing Group. doi:10.1038/s41558-022-01485-4.
URL <https://www.nature.com/articles/s41558-022-01485-4>
- [34] D. H. Meadows, D. Wright, Thinking in systems: a primer, Earthscan, London, 2009.
- [35] J. Sterman, Business dynamics, system thinking and modeling for a complex world, [http://lst-iiiep.iiep-unesco.org/cgi-bin/wwwi32.exe/\[in=epidoc1.in\]/?t2000=013598/\(100\)19\(012000\)](http://lst-iiiep.iiep-unesco.org/cgi-bin/wwwi32.exe/[in=epidoc1.in]/?t2000=013598/(100)19(012000)).
- [36] The World Bank, World Bank Open Data.
URL <https://data.worldbank.org>
- [37] European Conference of Ministers of Transport, Managing the Fundamental Drivers of Transport Demand, OECD, 2003. doi:10.1787/9789282113776-en.
URL https://www.oecd.org/en/publications/managing-the-fundamental-drivers-of-transport-demand_9789282113776-en.html
- [38] S. Kim, J. Edmonds, J. Lurz, S. Smith, M. Wise, The objects framework for integrated assessment: Hybrid modeling of transportation, *The Energy Journal Hybrid Modeling* (2006) 63–92. doi:10.2307/23297046.
- [39] C. A. Gallet, H. Doucouliagos, The income elasticity of air travel: A meta-analysis, *Annals of Tourism Research* 49 (2014) 141–155. doi:https://doi.org/10.1016/j.annals.2014.09.006.
URL <https://www.sciencedirect.com/science/article/pii/S0160738314001145>
- [40] D. Hanson, T. Toru Delibasi, M. Gatti, S. Cohen, How do changes in economic activity affect air passenger traffic? the use of state-dependent income elasticities to improve aviation forecasts, *Journal of Air Transport Management* 98 (2022) 102147. doi:https://doi.org/10.1016/j.jairtraman.2021.102147.
URL <https://www.sciencedirect.com/science/article/pii/S0969699721001289>
- [41] B. Andrieu, Modelling energy dependencies : from raw materials to global health, phdthesis, Université Grenoble Alpes [2020-....] (Oct. 2023).
URL <https://theses.hal.science/tel-04416040>
- [42] M. Sommer, J. Dargay, D. Gately, Vehicle Ownership and Income Growth, Worldwide: 1960-2030, *The Energy Journal* 28 (2007) 143–170. doi:10.2307/41323125.
- [43] A. Vedantham, M. Oppenheimer, Aircraft Emissions and the Global Atmosphere, Tech. Rep. 56, Environmental Defense Fund (1994).
URL <https://repository.upenn.edu/handle/20.500.14332/38468>
- [44] T. Planès, S. Delbecq, V. Pommier-Budinger, E. Bénard, Simulation and evaluation of sustainable climate trajectories for aviation, *Journal of Environmental Management* 295 (2021) 113079. doi:10.1016/j.jenvman.2021.113079.
URL <https://www.sciencedirect.com/science/article/pii/S0301479721011415>
- [45] T. J. Wallington, M. Woody, G. M. Lewis, G. A. Keoleian, E. J. Adler, J. R. Martins, M. D. Collette, Green hydrogen pathways, energy efficiencies, and intensities for ground, air, and marine transportation, *Journal of Energy* 8 (8) (2024) 2190–2207. doi:10.1016/j.joule.2024.07.012.
URL <https://linkinghub.elsevier.com/retrieve/pii/S2772656324000114>

- S2542435124003416
- [46] International Air Transport Association (IATA), Aircraft Technology Roadmap to 2050, Tech. rep., International Air Transport Association (2022).
URL <https://www.iata.org/en/programs/environment/roadmaps/>
- [47] Aircraft Technology Institute (ATI), Aerodynamic Structures Roadmap Report, Tech. rep., Aircraft Technology Institute (2022).
URL <https://www.ati.org.uk/wp-content/uploads/2022/03/FZO-AIR-COM-0016-Aerodynamic-Structures-Roadmap-Report.pdf>
- [48] Aircraft Technology Institute (ATI), Cryogenic Hydrogen Fuel System and Storage Roadmap Report, Tech. rep., Aircraft Technology Institute (2022).
URL <https://www.ati.org.uk/wp-content/uploads/2022/03/FZO-PPN-COM-0027-Cryogenic-Hydrogen-Fuel-System-and-Storage-Roadmap-Report.pdf>
- [49] Aircraft Technology Institute (ATI), Electrical Propulsion Systems Roadmap Report, Tech. rep., Aircraft Technology Institute (2022).
URL <https://www.ati.org.uk/wp-content/uploads/2022/03/FZO-PPN-COM-0030-Electrical-Propulsion-Systems-Roadmap-Report.pdf>
- [50] Aircraft Technology Institute (ATI), Fuel Cells Roadmap Report, Tech. rep., Aircraft Technology Institute (2022).
URL <https://www.ati.org.uk/wp-content/uploads/2022/03/FZO-PPN-COM-0033-Fuel-Cells-Roadmap-Report.pdf>
- [51] J. L. Felder, NASA Electric Propulsion System Studies, nTRS Author Affiliations: NASA Glenn Research Center NTRS Meeting Information: EnergyTech 2015; 2015-11-30 to 2015-12-02; undefined NTRS Report/Patent Number: GRC-E-DAA-TN28410 NTRS Document ID: 20160009274 NTRS Research Center: Glenn Research Center (GRC) (Nov. 2015).
URL <https://ntrs.nasa.gov/citations/20160009274>
- [52] K. V. Papatthakis, NASA Armstrong Flight Research Center Distributed Electric Propulsion Portfolio, and Safety and Certification Considerations, nTRS Author Affiliations: NASA Armstrong Flight Research Center NTRS Meeting Information: EýFlight Symposium; 2017-10-05 to 2017-10-06; undefined NTRS Report/Patent Number: AFRC-E-DAA-TN46675 NTRS Document ID: 20170009874 NTRS Research Center: Armstrong Flight Research Center (AFRC) (Oct. 2017).
URL <https://ntrs.nasa.gov/citations/20170009874>
- [53] A. Woodworth, NASA's Electric Aircraft Propulsion Research: Yesterday, Today and Tomorrow, nTRS Author Affiliations: Glenn Research Center NTRS Meeting Information: IEEE Workshop on Power Electronics for Aerospace Applications; 2023-07-18 to 2023-07-19; undefined NTRS Document ID: 20230008891 NTRS Research Center: Glenn Research Center (GRC).
URL <https://ntrs.nasa.gov/citations/20230008891>
- [54] M. K. Bradley, C. K. Droney, Subsonic Ultra Green Aircraft Research: Phase 2, Tech. Rep. NF1676L-21005, NASA, nTRS Author Affiliations: Boeing Research and Technology NTRS Document ID: 20150017039 NTRS Research Center: Langley Research Center (LaRC) (Apr. 2015).
URL <https://ntrs.nasa.gov/citations/20150017039>
- [55] E. U. A. S. A. (EASA), EASA.E.234 - E-811 Engine | EASA.
URL <https://www.easa.europa.eu/en/document-library/type-certificates/engine-cs-e/easae234-e-811-engine>
- [56] J. Beevor, K. Alexander, Missed targets: A brief history of aviation climate targets of the early 21st century, Tech. rep., Green Gumption for Possible (May 2022).
URL <https://www.wearepossible.org/our-reports/missed-target-a-brief-history-of-aviation-climate-targets>
- [57] Y. A. Kambiri, T. Druot, P. Roches, N. Peteilh, N. Monrolin, X. Carbonneau, Energy consumption of Aircraft with new propulsion systems and storage media, in: AIAA SCITECH 2024 Forum, American Institute of Aeronautics and Astronautics, Orlando, FL, 2024. doi:10.2514/6.2024-1707.
URL <https://arc.aiaa.org/doi/10.2514/6.2024-1707>
- [58] A. Salgas, J. Sun, S. Delbecq, T. Planès, G. Lafforgue, Compilation and applications of an open-source dataset on global air traffic flows and carbon emissions, Journal of Open Aviation Science 2 (1) (Jul. 2024).
- [59] I. Consulting, Estimating air travel demand elasticities, Tech. rep., The International Air Transport Association (IATA) (Dec. 2007).
URL <https://www.iata.org/en/iata-repository/publications/economic-reports/estimating-air-travel-demand-elasticities---by-intervistas/>
- [60] L. Goulder, R. Williams, The Choice of Discount Rate for Climate Change Policy Evaluation, Tech. Rep. w18301, National Bureau of Economic Research, Cambridge, MA (Aug. 2012). doi:10.3386/w18301.
URL <http://www.nber.org/papers/w18301.pdf>
- [61] D. Schoemaker, W. Schramade, Which discount rate for sustainability?, Journal of Sustainable Finance and Accounting 3 (2024) 100010. doi:10.1016/j.josfa.2024.100010.
URL <https://linkinghub.elsevier.com/retrieve/pii/S2950370124000105>
- [62] S. Delbecq, T. Planès, M. Delavenne, V. Pommier-Budinger, A. Joksimović, Aircraft fleet models using a bottom-up approach for simulating aviation technological prospective scenarios, in: 33rd Congress of the International Council of the Aeronautical Sciences, Stockholm, Sweden, 2022.
URL <https://hal.science/hal-03824184>
- [63] L. Jing, H. M. El-Houjeiri, J.-C. Monfort, J. Littlefield, A. Al-Qahtani, Y. Dixit, R. L. Speth, A. R. Brandt, M. S. Masnadi, H. L. MacLean, W. Peltier, D. Gordon, J. A. Bergerson, Understanding variability in petroleum jet fuel life cycle greenhouse gas emissions to inform aviation decarbonization, Nature Communications 13 (1) (2022) 7853. doi:10.1038/s41467-022-35392-1.
URL <https://www.nature.com/articles/s41467-022-35392-1>
- [64] R. W. Stratton, P. J. Wolfe, J. I. Hileman, Impact of Aviation Non-CO2 Combustion Effects on the Environmental Feasibility of Alternative Jet Fuels, Environmental Science & Technology 45 (24) (2011) 10736–10743, publisher: American Chemical Society. doi:10.1021/es2017522.
URL <https://doi.org/10.1021/es2017522>
- [65] U. Neuling, M. Kaltschmitt, Techno-economic and environmental analysis of aviation biofuels, Fuel Processing Technology 171 (2018) 54–69. doi:https://doi.org/10.1016/j.fuproc.2017.09.022.
URL <https://www.sciencedirect.com/science/article/pii/S0378382017307828>
- [66] M. Ji, J. Wang, Review and comparison of various hydrogen production methods based on costs and life cycle impact assessment indicators, International Journal of Hydrogen Energy 46 (78) (2021) 38612–38635. doi:https://doi.org/10.1016/j.ijhydene.2021.09.142.
URL <https://www.sciencedirect.com/science/article/pii/S0360319921036697>
- [67] A. Mendoza Beltran, B. Cox, C. Mutel, D. P. Van Vuuren, D. Font Vivanco, S. Deetman, O. Y. Edelenbosch, J. Guinée, A. Tukker, When the Background Matters: Using Scenarios from Integrated Assessment Models in Prospective Life Cycle Assessment, Journal of Industrial Ecology 24 (1) (2020) 64–79. doi:10.1111/jiec.12825.
URL <https://onlinelibrary.wiley.com/doi/10.1111/jiec.12825>
- [68] R. Sacchi, T. Terlouw, K. Siala, A. Dirnaichner, C. Bauer, B. Cox, C. Mutel, V. Daioglou, G. Luderer, Prospective environmental impact assessment (premise): A streamlined approach to producing databases for prospective life cycle assessment using integrated assessment models, Renewable and Sustainable Energy Reviews 160 (2022) 112311. doi:https://doi.org/10.1016/j.rser.2022.112311.
URL <https://www.sciencedirect.com/science/article/pii/S136403212200226X>
- [69] R. Sacchi, V. Becattini, P. Gabrielli, B. Cox, A. Dirnaichner, C. Bauer, M. Mazzotti, How to make climate-neutral aviation fly, Nature Communications 14 (1) (2023) 3989, publisher: Nature Publishing Group. doi:10.1038/s41467-023-39749-y.
URL <https://www.nature.com/articles/s41467-023-39749-y>
- [70] A. Bjørn, K. Richardson, M. Z. Hauschild, A Framework for Development and Communication of Absolute Environmental Sustainability Assessment Methods, Journal of Industrial Ecology 23 (4) (2019) 838–854, _eprint: <https://onlinelibrary.wiley.com/doi/pdf/10.1111/jiec.12820>. doi:10.1111/jiec.12820.
URL <https://onlinelibrary.wiley.com/doi/abs/10.1111/jiec.12820>

- [71] A. W. Hjalsted, A. Laurent, M. M. Andersen, K. H. Olsen, M. Ryberg, M. Hauschild, Sharing the safe operating space: Exploring ethical allocation principles to operationalize the planetary boundaries and assess absolute sustainability at individual and industrial sector levels, *Journal of Industrial Ecology* 25 (1) (2021) 6–19, [_eprint: https://onlinelibrary.wiley.com/doi/pdf/10.1111/jiec.13050](https://onlinelibrary.wiley.com/doi/pdf/10.1111/jiec.13050). doi:10.1111/jiec.13050.
URL <https://onlinelibrary.wiley.com/doi/abs/10.1111/jiec.13050>
- [72] B. Païs, A. Gondran, L. Hamelin, F. Simatos, Current aviation roadmaps are not within planetary boundaries (Nov. 2024). doi:10.21203/rs.3.rs-5409598/v1.
URL <https://www.researchsquare.com/article/rs-5409598/v1>
- [73] L. Clarke, Y.-M. Wei, A. D. L. V. Navarro, A. Garg, A. Hahmann, S. Khennas, I. Azevedo, A. Löschel, A. Singh, L. Steg, G. Strbac, K. Wada, Energy systems, in: Intergovernmental Panel On Climate Change (IPCC) (Ed.), *Climate Change 2022 - Mitigation of Climate Change*, 1st Edition, Cambridge University Press, 2023, Ch. 6, pp. 1049–1160. doi:10.1017/9781009157926.008.
URL https://www.cambridge.org/core/product/identifier/9781009157926%23c6/type/book_part
- [74] IEA, Share of oil final consumption by sector, 2019 – Charts – Data & Statistics (2021).
URL <https://www.iea.org/data-and-statistics/charts/share-of-oil-final-consumption-by-sector-2019>
- [75] R. D. Lamboll, Z. R. J. Nicholls, C. J. Smith, J. S. Kikstra, E. Byers, J. Rogelj, Assessing the size and uncertainty of remaining carbon budgets, *Nature Climate Change* 13 (12) (2023) 1360–1367, publisher: Nature Publishing Group. doi:10.1038/s41558-023-01848-5.
URL <https://www.nature.com/articles/s41558-023-01848-5>
- [76] ATAG, Powering global economic growth, employment, trade links, tourism and support for sustainable development through air transport, *Tech. rep., Aviation Benefits Beyond Borders* (2024).
URL https://aviationbenefits.org/media/xfmorflq/abbb2024_full-report.pdf
- [77] J. R. R. A. Martins, A. Ning, *Engineering Design Optimization*, Cambridge University Press, Cambridge, UK, 2022. doi:10.1017/9781108980647.
URL <https://mbook.github.io>
- [78] F. Gallard, C. Vanaret, D. Guenot, V. Gachelin, R. Lafage, B. Pauwels, P.-J. Barjhoux, A. Gazaix, GEMS: A Python Library for Automation of Multidisciplinary Design Optimization Process Generation, in: 2018 AIAA/ASCE/AHS/ASC Structures, Structural Dynamics, and Materials Conference, American Institute of Aeronautics and Astronautics, Kissimmee, Florida, 2018. doi:10.2514/6.2018-0657.
URL <https://arc.aiaa.org/doi/10.2514/6.2018-0657>
- [79] J. Bradbury, R. Frostig, P. Hawkins, M. J. Johnson, C. Leary, D. Maclaurin, G. Necula, A. Paszke, J. VanderPlas, S. Wanderman-Milne, Q. Zhang, JAX: composable transformations of Python+NumPy programs (2018).
URL <http://github.com/google/jax>
- [80] I. Costa-Alves, F. Gallard, M. De Lozzo, A. Dechaume, Overview - gemseo-jax.
URL <https://gemseo-jax-gemseo-dev-ab34b8978a329997ad18a32395ac187acf263c40b.gitlab.io/develop/>
- [81] D. Kraft, A Software Package for Sequential Quadratic Programming, Deutsche Forschungs- und Versuchsanstalt für Luft- und Raumfahrt Köln: Forschungsbericht, *Wiss. Berichtswesen d. DFVLR*, 1988.
URL https://degenerateconic.com/uploads/2018/03/DFVLR_FB_88_28.pdf
- [82] V. D. Blondel, J. L. Guillaume, R. Lambiotte, E. Lefebvre, Fast unfolding of communities in large networks, *J. Stat. Mech.-Theory Exp.* 2008 (2008) P10008.
- [83] On a bicriterion formulation of the problems of integrated system identification and system optimization, *IEEE Transactions on Systems, Man, and Cybernetics SMC-1* (3) (1971) 296–297. doi:10.1109/TSMC.1971.4308298.
- [84] R. E. Perez, P. W. Jansen, J. R. R. A. Martins, pyOpt: a Python-based object-oriented framework for nonlinear constrained optimization, *Structural and Multidisciplinary Optimization* 45 (1) (2012) 101–118. doi:10.1007/s00158-011-0666-3.
URL <http://link.springer.com/10.1007/s00158-011-0666-3>
- [85] C. Mourouzidis, G. Singh, X. Sun, J. Huete, D. Nalianda, T. Nikolaidis, V. Sethi, A. Rolt, E. Goodger, P. Pilidis, Abating CO₂ and non-CO₂ emissions with hydrogen propulsion, *The Aeronautical Journal* 128 (1325) (2024) 1576–1593. doi:10.1017/aer.2024.20.
URL https://www.cambridge.org/core/product/identifier/S0001924024000204/type/journal_article
- [86] S. Drünert, U. Neuling, T. Zitscher, M. Kaltschmitt, Power-to-Liquid fuels for aviation – Processes, resources and supply potential under German conditions, *Applied Energy* 277 (2020) 115578. doi:10.1016/j.apenergy.2020.115578.
URL <https://linkinghub.elsevier.com/retrieve/pii/S0306261920310904>
- [87] K. Riahi, R. Schaeffer, J. Arango, K. Calvin, C. Guivarch, T. Hasegawa, K. Jiang, E. Kriegler, R. Matthews, G. Peters, A. Rao, S. Robertson, A. Sebbit, J. Steinberger, M. Tavoni, D. van Vuuren, Energy systems, in: Intergovernmental Panel On Climate Change (IPCC) (Ed.), *Climate Change 2022 - Mitigation of Climate Change*, 1st Edition, Cambridge University Press, 2023, Ch. 6, pp. 1049–1160. doi:10.1017/9781009157926.008.
URL https://www.cambridge.org/core/product/identifier/9781009157926%23c6/type/book_part
- [88] S. Gössling, A. Humpe, The global scale, distribution and growth of aviation: Implications for climate change, *Global Environmental Change* 65 (2020) 102194. doi:https://doi.org/10.1016/j.gloenvcha.2020.102194.
URL <https://www.sciencedirect.com/science/article/pii/S0959378020307779>
- [89] G. of Brazil: Ports, Airports, Voa brasil: the first social inclusion program in brazilian aviation.
URL <https://www.gov.br/portos-e-aeropostos/pt-br/assuntos/conheca-o-voa-brasil>
- [90] M. Büchs, G. Mattioli, How socially just are taxes on air travel and ‘frequent flyer levies’?, *Journal of Sustainable Tourism* 32 (1) (2024) 62–84. arXiv:https://doi.org/10.1080/09669582.2022.2115050, doi:10.1080/09669582.2022.2115050.
URL <https://doi.org/10.1080/09669582.2022.2115050>
- [91] J. Rockström, W. Steffen, K. Noone, A. Persson, F. S. Chapin, E. F. Lambin, T. M. Lenton, M. Scheffer, C. Folke, H. J. Schellnhuber, B. Nykvist, C. A. De Wit, T. Hughes, S. Van Der Leeuw, H. Rodhe, S. Sörlin, P. K. Snyder, R. Costanza, U. Svedin, M. Falkenmark, L. Karlberg, R. W. Corell, V. J. Fabry, J. Hansen, B. Walker, D. Liverman, K. Richardson, P. Crutzen, J. A. Foley, A safe operating space for humanity, *Nature* 461 (7263) (2009) 472–475. doi:10.1038/461472a.
URL <https://www.nature.com/articles/461472a>
- [92] K. Richardson, W. Steffen, W. Lucht, J. Bendtsen, S. E. Cornell, J. F. Donges, M. Drüke, I. Fetzer, G. Bala, W. Von Bloh, G. Feulner, S. Fiedler, D. Gerten, T. Gleeson, M. Hofmann, W. Huiskamp, M. Kumm, C. Mohan, D. Nogués-Bravo, S. Petri, M. Porkka, S. Rahmstorf, S. Schaphoff, K. Thonicke, A. Tobian, V. Virkki, L. Wang-Erlandsson, L. Weber, J. Rockström, Earth beyond six of nine planetary boundaries, *Science Advances* 9 (37) (2023) eadh2458. doi:10.1126/sciadv.adh2458.
URL <https://www.science.org/doi/10.1126/sciadv.adh2458>